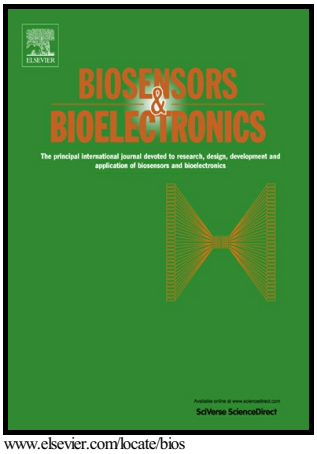

www.elsevier.com/locate/bios

Evolving trends in bio/chemical sensors fabrication incorporating bimetallic nanoparticles

Riddhipratim Mandal, Anupriya Baranwal, Ananya Srivastava, Pranjal Chandra

PII: S0956-5663(18)30471-8
DOI: https://doi.org/10.1016/j.bios.2018.06.039
Reference: BIOS10559

To appear in: *Biosensors and Bioelectronic*

Received date: 24 April 2018
Revised date: 16 June 2018
Accepted date: 20 June 2018

Cite this article as: Riddhipratim Mandal, Anupriya Baranwal, Ananya Srivastava and Pranjal Chandra, Evolving trends in bio/chemical sensors fabrication incorporating bimetallic nanoparticles, *Biosensors and Bioelectronic,* https://doi.org/10.1016/j.bios.2018.06.039

Evolving trends in bio/chemical sensors fabrication incorporating bimetallic nanoparticles

Riddhipratim Mandal[1], Anupriya Baranwal[1], Ananya Srivastava[2], Pranjal Chandra[1*]

[1]Department of Biosciences and Bioengineering, Indian Institute of Technology Guwahati, Guwahati-781039, Assam, India

[2]Department of Pharmacology and Toxicology, National Institute of Pharmaceutical Education and Research, Guwahati, 781006, Assam, India

[*]**Corresponding author.** Tel.: +91-361-258-3207; fax: +91-361-258-2249. pchandra13@iitg.ernet.in

Abstract

Biosensor designing took a giant leap in its path of evolution after its merger with a wing of nanotechnology. Dramatic properties like high surface area to volume ratio, enhanced chemical and optical properties of nanoscale materials have revolutionized sensor technology in terms of their analytical performance. Many metallic nanoparticles (MeNPs) like gold, silver, platinum, palladium nanoparticles, *etc.* have been tremendously exploited for improving sensor performance. Over the years, there has been slow but steady shift in nanoscience research with an aim to explore composite MeNPs like bimetallic, trimetallic nanoparticles, *etc.* So far, these engineered nanoparticles are shown to possess multifunctional properties which are providing several advantages over monometallic nanoparticles (mono-NPs). As a result of these properties, composite MeNPs, particularly bimetallic nanoparticles (BNPs), have sought the attention of sensor engineers and since then there has been rapid rise in the number of reports of sensors incorporating BNPs within a brief period of time. Keeping this pivotal fact in consideration, we

have complied this review to give readers a clear insight in the possible ways BNPs can be synthesized that would render them to possess crucial characteristics desired for bio/chemical sensor fabrication and their applications. We have also discussed different characterization techniques that have been applied to investigate various properties of the BNPs along with a table that gives information on how each technique is different and in what ways they complement each other. Moreover, a comprehensive report on the incorporation of different BNPs in sensor fabrication for detection of hydrogen peroxide (H_2O_2), glucose, pesticides, nucleic acids, proteins, cancerous and bacterial cells has been described. The comparison of analytical performance of the biosensor design incorporating mono-NPs and BNPs, in terms of linear range (LR), limit of detection (LOD), sensitivity, and specificity, has also been discussed to show the importance of BNPs in sensing matrix.

Keywords: Bio/Chemical Sensors; Bimetallic nanoparticles; Analytical performance; Diagnostics; Material Engineering

1. Introduction

Nanoparticles have one or more dimensions in the nanometer range (1-100 nm) and properties that are different from the bulk material of the same chemical species (Bhushan, 2017; Chandra et al., 2010). The dramatic properties exhibited by these exceedingly small particles which continue to draw researchers' attention include electronic (Boyen et al., 2001; Mahato et al., 2018), catalytic (Cuenya, 2010; Noh et al., 2012), magnetic (Goya et al., 2003; Mørup et al., 2010), and optical properties (Chandra et al., 2013a; Kelly et al., 2003). A wide range of nanoparticles belonging from both organic and inorganic nanoparticles have been synthesized till date. MeNPs, a subclass of inorganic nanoparticles, have been of special interest for their potential applicability in diverse fields including applied electronics (Ko et al., 2007a; Ko et al., 2007b), genetic engineering (Ghosh et al., 2008a; Ghosh et al., 2008b), nanomedicine (Baranwal et al., 2018b; Chen et al., 2008), imaging (Prasad et al., 2016; Vellaisamy et al., 2018; Wang et al., 2017; Zhu et al., 2012b), and diagnostics from classical prototypes to modern lab-on chip systems (Chandra, 2016; Chandra et al., 2011; Choudhary et al., 2016; Chung et al., 2018; Hori

et al., 2018; Mahato et al., 2016; Wang et al., 2018). For their promising utility in these fields, mono-NPs have undergone extensive investigation in terms of their synthesis and characterization to understand their physico-chemical properties. Till today, mono-NPs of different metals like gold, silver, copper, cobalt, iron, platinum, *etc*. (Poole Jr and Owens, 2003) have been synthesized and used in various applications. Despite the immense utilities that mono-NPs offer, there is need to develop a superior class of nanoparticles with properties that are so far not reported. In this regard, BNPs could be a promising candidate for multifunctional characteristics as they are a combination of two different metals and hence possess great potential from both technological point as well as scientific exploration (Zaleska-Medynska et al., 2016). The possible occurrence of such novel properties in BNPs can be due to blending of the properties of the individual metals or synergy between the two metals. Synergy due to mixing of the two metals not only enhances the existing properties, but also gives rise to new characteristics (Gu et al., 2011; Wang et al., 2008). For example, alloy Au-Ag BNP shows strong synergistic effect in promoting the low-temperature oxidation of CO (Liu et al., 2005). This clearly suggests that the synergistic effect of mono-NPs present in the BNPs can give rise to improved catalytic properties which has also been utilized in oxidation of methanol, ethanol, formic acid, ammonia, etc. (Singh and Xu, 2013). Combination of properties of metals have been utilized to design multifunctional nanoparticles, for instance, opto-magnetic nanoparticles (Bao et al., 2007; Lee and Chen, 2006), oxidation resistant nanoparticles (Plascencia et al., 2005), *etc.* From another point of view, shape and size of the nanoparticles are always a matter of interest, as crucial properties of nanoparticles like chemical activity, optical property, depend upon these parameters (Cuenya, 2010; Kelly et al., 2003). For BNPs, a variety of architectures, such as core-shell, composite or alloy, clusters, multi-shells, *etc.* have been made, which have never been reported in any of the mono-NPs (Liu and Astruc, 2017; Nasrabadi et al., 2016).

Biosensing is an applied, interdisciplinary field of engineering encompassing biological sciences (Agrawal et al., 2013), chemistry (Chandra et al., 2012), electronics (Pallela et al., 2016), optics (Zhu et al., 2012a), and mechanics (Schürmann et al., 2016), for developing diagnostic devices for medical purposes as well as environmental monitoring (Mahato et al., 2017; Mahato et al., 2018). A typical biosensor mainly consists of a bio-recognition element (BRE), transducer, amplifier, and a detector. Interaction of BRE with its target analyte generates a signal for the transducer which converts it into a readable signal. Depending on the type of

transducer, biosensor is classified under optical, electrochemical, electromechanical, and calorimetric types. These biosensors differ in terms of their biosensing mechanism which has been described elsewhere (Chandra, 2016). Ever since the idea of developing sensors has been adopted, there have been constant endeavors to improve sensor performance in terms of specificity and sensitivity. The specificity issues have been resolved by incorporating BREs; however, the sensitivity issues have been resolved by exploiting novel materials in electrode fabrication (Turner, 2013). Use of mono-NPs, in the direction of sensitivity enhancement has revolutionized the sensing technology, yet the need for further fine tuning and enhancing the sensor performance still persists. Therefore, new classes of engineered nanoparticles like bimetallic, trimetallic, composite nanoparticles, *etc*. are being tried for sensing applications. At present, other multimetalic nanosystems, such as trimetallic and tetrametallic, *etc*. are in nascent stage for their prospective sensing applications.

Fabrication of BNPs is a new and enterprising area of research. The full potential of this class of nanoparticles is yet to be explored and thereafter harnessed, as a vast array of metal combinations is possible. However, due to rapid investigation of BNPs, the amount of data that has already been accumulated in the brief period of research is substantial and scientifically significant. We surveyed the existing literature on BNPs and in this review and have tried to present a tutorial with holistic approach to BNPs based biosensors. We have discussed BNP synthesis followed by a systematic discussion on different synthetic approaches. We have also documented various characterization techniques for the synthesized BNPs including the ones which are essential to confirm their formation. Furthermore, the application of such BNPs in biosensing domain has been discussed elaborately for the detection of various targets, such as H_2O_2, glucose, cholesterol, pesticides, nucleic acids, peptides, cancerous and bacterial cells. The analytical performance of the sensors in terms of sensitivity, selectivity, LR, LOD have been incorporated comprehensively. Also, the comparison of analytical performance of sensors incorporating mono-NPs and BNPs have been discussed.

2. Synthetic procedures for designing bimetallic nanoparticles

It is important to have the elementary knowledge of the underlying principles of mono-NPs designing in order to understand the different synthetic approaches designed for BNPs. BNPs, as they are made from two different metals (Toshima and Yonezawa, 1998), their mode of synthesis

is often a modification or extension of the procedures used for the synthesis of their monometallic counterparts, separately. Ever since the advent of nanotechnology, mono-NPs have been synthesized either by top-down or bottom-up approach (Chandra et al., 2013b). In top-down approach, metals are demolished or disintegrated from bulk into particles of nanometer dimension and in bottom-up approach, nanometer sized particles are built from ions or atoms. Both the strategies have been extensively employed; however, bottom up approaches are more widely accepted due to the various advantages, including their capability of producing monodisperse particles of tunable structure, and less-energy intensive operations (Bhushan, 2010). For synthesis of mono-NPs using bottom up approach, usually metal salts are used as the starting materials. In the aqueous phase, metals possess non-zero oxidation state and hence are in ionic form. An electron donor commonly known as a reducing agent is used to bring these ions into zero-valent state forming the mono-NPs. Different molecules including inorganic (*viz.* $NaBH_4$, *etc.*); or organic (*viz.* polyalcohol, carbohydrates, proteins, *etc.*) moieties (Chandra et al., 2015; Zhu et al., 2012b; Zhu et al., 2012c) can be used as a reducing agent. Despite being extensions of MNP synthesis, the approaches for BNP synthesis consist of subtle differences due to the architecture of the particles and the arrangements of the constituent metals in them (Alayoglu and Eichhorn, 2008). Following primarily the bottom up approach, the most reported bimetallic nanostructures are achieved by simultaneous reduction or sequential reduction depending on the choice of arrangement and distribution of metals within the particles (Tojo et al., 2017). Both chemical as well as physical techniques have been reported for either of the above-mentioned modes of reduction. The synthetic procedures of BNP synthesis have been classified majorly under three categories, chemical, physical, and biological methods as indicated in the following sections.

2.1 Chemical methods

Synthesis of BNPs by chemical approaches involve bottom up strategy and thus, synthesis by chemical routes involve building up the particles by aggregation of reduced metal ions (Akdim et al., 2013). The participating metal salts, in solution phase, are reduced either in succession or simultaneously in the presence of a chemical reducing agent which acts as an electron donor. The

reduction is followed by the aggregation of the metal atoms forming stabilized BNPs. In sequential reduction, which is shown in **figure 1 (A)**, one metal is reduced followed by the other, where the metal that is reduced first forms the seed, upon which the other metal aggregates. The sequential combination of solvents can be either aqueous-aqueous, aqueous-organic, or organic-organic (Ghosh Chaudhuri and Paria, 2011). This method is preferred for obtaining core-shell strcuture of BNPs (one metal is coated by another metal) (Lin et al., 2001). In simultaneous reduction, both the metal ions are reduced together, usually in a single solvent (Zhang et al., 2007) which is shown in **figure 1 (B)** . This is usually possible for the choice of metals whose reduction kinetics do not differ much. This method usually favors the formation of composite BNPs which have a fairly even distribution of both the metals within a particle. Chemical synthesis often involves use of stabilising agents, which coat the nanoparticles to prevent uneven aggregation and therefore, control the size of the nanoparticles. The stabilizing agents used for the purpose usually include polymers like chitosan, nafion, polylactic glycolic acid, *etc.*

2.1.1 Methods based on chemical reduction

So far, various methods based on chemical reduction have been used for the synthesis of BNPs. The chemistry behind this method is reduction of metallic ions to zero-valent metal atoms from the electrons donated by the reducing agent; such as, sodium borohydride, ascorbic acid, citric acids, hydrazine, sodium hydroxide, *etc.* (Ghosh Chaudhuri and Paria, 2011). In addition to these, hydrogen gas has also been used as a reducing agent. For instance, Pt-Cu and Pd-Cu BNPs were obtained by spreading the corresponding salts on activated carbon, followed by their reduction in hydrogen atmosphere (Barrabés et al., 2006).

2.1.2 Methods based on micro-emulsion system

BNPs have also been synthesized using micro-emulsion system employing phase separation to obtain the reduced metal ions, which eventually forms the particles. A typical micro-emulsion system usually comprises of a polar phase, a nonpolar phase, and a surfactant. The surfactant acts as a barrier or a separating boundary between the two phases. Among all polar and non-polar emulsions, water-in-oil based system is most commonly used for BNP synthesis (Zhang and Chan, 2003). This system facilitates aggregation of reduced bimetal atoms inside the close boundary of droplets of sub-nanometers range (Balint et al., 2002; Han et al., 2008). In these systems, the size of synthesized nanoparticles depends on various factors, *viz.* ratio of the phases,

concentration of the reagents, and surfactants (Ahmed et al., 2009; Santra et al., 2001). For the BNP synthesis, mainly three types of methods have been employed, which include micro-emulsion-micro-emulsion; micro-emulsion-aqueous, and micro-emulsion-gaseous method (Ahmed et al., 2009; Balint et al., 2002). In every method, the metallic salts are kept in micro-emulsion phase while the reducing agents are kept in the different phase. In a recent report, Pt-Au BNPs were synthesized by depositing them on multi-walled carbon nanotubes (MWCNTs) using micro-emulsion method (Félix-Navarro et al., 2016). These BNPs were shown to exhibit excellent electrocatalytic activity for the reduction of oxygen. Keeping this application in consideration, it could be interesting to extend such work further and design a sensor for the detection of oxygen and other gaseous molecules.

2.2 Physical methods

Like chemical reduction methods, BNPs have also been generated by using physical methods. It may be said to involve disintegrating the metal from bulk to nanoscale, which is what exactly happens in vapor deposition (Hierso et al., 1998; Swihart, 2003). Other than this, there are methods which involve physical agents like radiation to bring out BNP synthesis. Physical methods involving bottom up approach are discussed as follows:

2.2.1 Photo-deposition method

Photo-deposition is the most commonly used method to modify semiconductors by loading BNPs upon them (Wenderich and Mul, 2016). This process of loading BNPs on semiconductor surface is mediated by electrons generated by ultra-violet radiations. There are reports of noble metals like Au, Ag, Pt, and Pd to be deposited with high efficiency using photo-deposition method. There are two different approaches for bringing out photo-deposition onto semiconductor surface (i) simultaneous and (ii) successive photo-deposition. It is reported that with successive deposition, there is formation of separate layers on the surface of the semiconductor. This is however, not a problem with simultaneous deposition, as BNPs settle in the form of alloy-coat upon the semiconductors. Therefore, this method can also be used to perform site specific deposition of the nanoparticles onto semiconductor surface and other metals as well. Using this technique, Pt-TiO_2 BNPs have been developed, possessing photocatalytic activity towards oxidation of dichloroacetic acid (Ismail and Bahnemann, 2011).

2.2.2 Radiolysis

In this method, high energy radiation like gamma (γ) or X-rays or even ionic rays like electrons are used to break down alcohol in order to generate free radicals. These free organic radicals are highly reactive in nature and act as strong reducing agents. By using γ-radiation Pd-Pt BNPs have been designed to fabricate a nitrogen dioxide sensor (Choi et al., 2013). Besides alloy nanoparticles, core shell structure can also be prepared by this method. The structure and the arrangement of metals in BNPs can be controlled by monitoring the dosage of γ-radiation (Remita et al., 2003). The γ-radiation dose dependent synthesis of BNPs has been shown in **figure 2**. It has been reported, that core shell structure can be synthesized by giving low dosage of γ-radiation **(figure 2 (A)),** whereas alloyed nanoparticles can be synthesized by giving high dosage of γ-radiation **(figure 2 (B))** (Aaron et al., 2006).

2.3 Biological synthesis

Although aforementioned techniques are very powerful and have been widely used, they possess certain limitations which restrict their usage. Chemical methods, at times, require reagents which are harmful to both humans as well as environment. On the other hand, physical methods demand energy intensive procedures and sophisticated instrumentation which incur high cost investment (Mittal et al., 2014). Therefore, an alternative approach, which is ecofriendly and inexpensive, needs to be developed for BNP synthesis. In this direction, various biological approaches have been developed, where many plant tissue extracts have been used for this purpose. Presence of secondary metabolites like alkaloids, terpenoids, flavones, phenolic *etc.* in the plant tissue make it suitable to act as reducing as well as stabilizing agent (Baranwal et al., 2016; Baranwal et al., 2018). There have been several reports on synthesis of mono-NPs using plant extracts (Ahmed et al., 2016); however, synthesis of BNPs using plant extracts have been relatively less reported. Some of the plant extracts that have been used for synthesizing BNPs are obtained from *Punica granatum* (Kumari et al., 2015), *Piper pedicellatum* (Tamuly et al., 2013), *Anacardium occidentale* (Sheny et al., 2011), mahogany leaves (Mondal et al., 2011), *Azadirachta indica* (Shankar et al. 2004). Using these examples, it has to be mentioned that primarily Au-Ag BNPs are synthesised and other combinations of BNPs are rarely reported. This shows that there is scope to explore other metal combinations as well. Also, phytofabricated

BNPs have been exploited for very limited applications and therefore, more work could be directed towards phytosynthesis BNPs which have potential to be used in sensing application.

After critical study of the aforementioned methods of BNP syntheses, we have drawn a comparison between advantages and disadvantages of each approach and tabulated them in **table 1** and schematically shown the same in **figure 3**.

3. Characterization of bimetallic nanoparticles

In order to understand different properties of BNPs, several characterization techniques **(figure 4)** have been employed which has been reported elsewhere (Astruc, 2008). UV-Visible spectroscopic technique has been used to ensure the presence of two metals in a BNP, based on the shift in absorption maxima of the BNPs from those of their constituent mono-NPs. Confirmation of BNP synthesis is brought out by elemental mapping linked transmission electron microscopy (TEM) of these particles, where the metal constituents and their arrangement can be elucidated. Investigation of nanoparticles' size and morphology is very critical for their application in various biomedical and therapeutic domains and to elucidate these parameters scanning electron microscopy and TEM have been used. Additionally, these microscopy techniques assist in understanding the dispersity of BNPs. Dynamic light scattering is a technique which has been used to investigate the hydrodynamic radius and polydispersity of BNPs. The molecular compactness, crystallinity, and lattice parameters are major contributors to estimate the mechanical, optoelectronic, and magnetic properties of BNPs. In order to investigate such properties, X-ray diffractographic analysis is employed. Another technique to give similar information is selective area electron diffraction. A large number of other techniques have been used for the characterization of these BNPs which are mentioned in **table 2** and some of these techniques are indispensable for characterizing BNPs **(table 2 a).**

4. Bimetallic nanoparticles for sensing applications

Owing to their unique properties mentioned in introduction section, BNPs are undergoing extensive investigation for their application in various domains. Of these properties, catalysis is particularly noteworthy, as they have been reported to exhibit better catalytic efficiency than most mono-NPs (Sankar et al., 2012; Zaleska-Medynska et al., 2016). Presence of two different metals within a bimetallic nanosystem often have a synergistic effect due to complementation of

their individual catalytic properties. Several combinations of metals, such as Pt-Co (Park et al., 2008; Wang et al., 2014), Au-Pd (Mizukoshi et al. 2000), Rh-Pt (Park et al. 2008), Au-Pt (Suntivich et al. 2013), *etc.* have been reported to have this property. The property of enhanced catalytic effect of BNPs is besides investigation, being utilized to design various sensors targeting different types of chemical and biological samples. In addition to this, BNPs have also been shown to exhibit improved localized surface plasmon resonance (Abraha, 2016; Ghodselahi et al., 2014) and enhanced magnetic properties (Cai et al., 2016), which make them potential candidate material for designing robust and highly sensitive sensors. Not only this, BNP based biosensors show better analytical performance due to great ease in electron transfer as compared to that of mono-NPs based biosensors (Ghodselahi et al., 2014). The surface area dependent tunable electrocatalytic activity of the BNPs is also one of the factors for having better performing sensors (Gan et al.,2018). In recent years, there has been rise in the number of reports on sensor development employing BNPs, which clearly shows the change in trend with this emerging class of engineered nanomaterials. BNP based biosensors have been developed for detection of small molecules like glucose, free radicals like H_2O_2, large biological macromolecules like nucleic acids and proteins, and whole cells like cancer and bacterial cells. Keeping this pivotal fact in consideration, the following section is dedicated towards providing an insight into various examples of biosensors incorporating BNPs for the detection of numerous analytes.

4.1 Sensing of hydrogen peroxide

Detection of H_2O_2 is extremely important as it has great significance in biological matrices and can aid in diagnosing different clinical/pharmacological conditions. In this direction, Gowthaman *et al.* prepared Au-Ag BNPs in a sequential reduction reaction and studied the varying Au:Ag concentrations for efficient electrochemical detection of H_2O_2 (Gowthaman et al., 2016). The glassy carbon electrode (GCE) modified with previously synthesized Au-Ag BNPs in 1: 0.12 Ag:Au ratio resulted in a sensing probe with highest analytical performance. This novel sensing probe resulted sensitive detection of H_2O_2 with a LOD of 0.12 μM. In another report, Ko *et al.* synthesized a microfluidic biosensor based on Au-Ag BNPs for the electrochemical detection of H_2O_2 (Ko et al., 2017). The working electrode of this sensor was fabricated by doping it with single walled carbon nanotubes (SWCNTs) and Au-Ag BNPs. This modified electrode was

shown to have good performance with a LOD of 26.8 μM. Interestingly, BNPs have not only been utilized for electrochemical sensing of H_2O_2, but they have also been employed for the optical sensing of H_2O_2. In one such example, Chen *et al.* developed a detection system for colorimetric H_2O_2 sensing using a non-noble metal based BNP of Fe-Co (Chen et al., 2013). The BNPs were utilized for their catalytic action on H_2O_2 reduction and thereby simultaneous oxidation of 3,3',5,5'-tetramethylbenzidine (TMB) which produced color that was observed by spectrometry **(figure 5 (A) and (B))**. In addition to the aforementioned BNPs for H_2O_2 detection, other metal combinations have also been designed, such as Au-Pt (Gowthaman et al., 2017), Pt-Ru (Kung et al., 2014), and Ru-Rh (Janasek et al., 2002), for highly efficient and robust analysis of H_2O_2 in various matrices.

In a classical H_2O_2 sensing, peroxidase enzyme based sensing systems have been tremendously studied; however, recently BNPs have been attempted for the detection of H_2O_2 in an enzyme-less sensing format for their high catalytic efficiency. For the utility and ease of reduction of H_2O_2, detection of other small molecules is being done with a coupling reaction, where an equivalent amount of H_2O_2 is produced. Classical analytical techniques often involve generation of chemically active species (such as H_2O_2), which is utilized in a coupling reaction to generate a color whose intensity is measurable or there is electron exchange due to reduction of H_2O_2, that can be channelized to generate an electrical signal. BNPs have given an alternative over using enzymes in these biosensor designs and therefore, enabled small molecule detection via. enzyme-less biosensors, some of which have been discussed in the following section.

4.2 Sensing of small organic molecules

Analysis of small organic molecules such as glucose, cholesterol, and pesticides (organophosphates) is of great importance in clinical diagnosis and environmental monitoring. In last few decades, numerous strategies have been accumulated for the detection of such molecules however, incorporation of BNPs in sensor matrix for the same purpose is relatively new. Few of the important BNPs for the detection of such molecules have been discussed in the following sections.

4.2.1 Sensing of glucose

These sensors made use of the classic enzyme glucose oxidase (GOD), which still remains the model enzyme for testing biosensor prototypes. With the merger of nanotechnology and sensing technology, MeNPs have led to the development of sensors with dramatic improvement in performance. Since then, many glucose biosensors have been developed. Of late, BNPs are being engineered for the same purpose as were mono-NPs. Owing to the enhanced catalytic activity of the BNPs, sensors operating on these parameters have been shown to have further improved analytical performance (Ghodselahi et al., 2014). Many reports have come up in the last decade on BNP based glucose biosensors. Kang *et al.* was one of the pioneering groups who developed BNP based electrochemical glucose biosensor (Kang et al., 2007). They developed a chitosan matrix which was immobilized with GOD enzyme and modified with Au-Pt BNPs deposited in carbon nanotubes (CNTs) in order to modify GCE. The developers claimed "biosensor exhibited excellent performances for glucose detection at a low applied potential (0.1 V)." The sensor was reported to be fast responding showing the LOD of 0.2 µM of glucose and a wide LR of 0.001 to 7.0 mM. In another study, Leng *et al.* synthesized the same bimetallic nanosystem for glucose sensing but they synthesized the nanoparticles through a different approach (Leng et al., 2014). They reported synthesis of the BNPs by using single stranded DNA as template which they immobilized onto graphene and upon this they assembled Pt-Au BNPs using hydrazine as reducing agent. DNA is used as a scaffold for high efficient synthesis of uniform and monodispersed BNP-graphene composite as the uniform stereochemistry and near regular repetition of functional groups in DNA could prevent formation of unevenness of the nanocomposite. GOD was immobilized onto this matrix and the entrapped enzyme was found to retain its activity for longer duration. They used this modified electrode to quantify glucose and found that this system had a LR of 1 to 1800 µM of glucose with an LOD of 0.3 µM. A Pt-Pd BNP based amperometric glucose biosensor has also been developed where, the BNPs were decorated upon MWCNTs in a facile experimental setting to form composite (Chen et al., 2012). This composite was coated on GCE followed by immobilization of GOD to obtain the final sensing probe. The construction of this biosensor and the sensing principle is shown in **figure 6 (A).** The enzyme modified system assisted through incorporating Pt-Pd BNPs resulted in a highly selective and sensitive glucose biosensor showing the LOD of 0.031 mM and wide LR between 0.062 and 14.07 mM. Another sensor was designed by Yang *et al.* for enzymatic detection of glucose but operating on a strategy slightly different from the above (Yang et al.,

2011). Au-Pd BNPs were synthesized electrochemically without using any chemical reducing agent which were used to dope rGO followed by immobilization of GOD. It was characterized using various techniques which made it evident that this system was particularly stable for oxygen reduction. This sensor, unlike the ones listed above, worked by monitoring the oxygen consumption level by GOD enzyme instead of H_2O_2 amount generated during the reaction. The LOD of this sensor for glucose was found to be 6.9 µM. There was another report, published by Li *et al.* on development of an enzyme-less glucose biosensor utilizing Ni-Cu BNPs modified titanium oxide nanotubes (Li et al., 2013b). These BNPs were involved in electrocatalytic oxidation of glucose which precluded the use of GOD enzyme. The presence of Ni in BNPs was found to be involved in redox coupling and thereby electron transport, by switching between $Ni(OH)_2$/NiOOH forms. This sensor, besides being enzyme-less, was resistant to chloride ion fouling which is a common problem faced with conventional sensing probes. Apart from this, the strategy followed by this group enabled inexpensive glucose detection as the metal salts used for designing BNPs were inexpensive compared to those bimetallic nanosystem which incorporated noble metals. Apart from electrochemical sensor, optical sensors have also been designed to enable glucose sensing. In a very recent report, a colorimetric sensor was designed for detection of glucose using Cu-Ag BNP modified reduced graphene oxide (rGO) electrode (Darabdhara et al., 2017). The strategy adopted, was fairly simple using a conventional procedure based on glucose oxidase/peroxidase (GOD-POD) method of glucose quantification. In this technique, glucose was oxidized by the enzyme GOD to gluconolactone and H_2O_2, and the produced free radical was utilized by the bimetallic nanosystem to oxidize TMB in order to produce a characteristic color of measurable intensity. In this report, the Cu-Ag BNPs mimicked the role of POD enzyme and resulted in successful detection of glucose with an LOD of 3.8 µM in human serum samples. In a comparative study, under similar experimental conditions, the LOD of glucose was found to be 9.7 µM and 7.9 µM when Cu and Ag mono-NPs were tested, respectively. Considerably lower LOD obtained for BNP clearly indicates its importance in the analytical performance of the designed biosensor.

4.2.2 Sensing of cholesterol

Cholesterol, an important biomarker related to various clinical conditions, has also been widely investigated for detection. So far, several materials are designed and utilized for cholesterol sensing (Saxena and Das, 2016); however, BNP based sensing has been relatively less reported. In one such example, Cao *et al.* modified a GCE with graphene and chitosan which were previously doped with Pt-Pd BNPs (Cao et al., 2013) for electrochemical detection of cholesterol. The fabrication strategy followed by this group has been shown in **figure 6 (B)**. Cholesterol oxidase (COX) enzyme was immobilized on the nanocomposite to obtain the final sensing probe. The LR for cholesterol detection was found to be between 2.2×10^{-6} and 5.2×10^{-4} M with an LOD of 0.75 µM. This system also had an additional advantage of high specificity for cholesterol and complete insulation from the noises coming from uric acid and glucose present in real samples. Safavi and Farjami designed another bimetallic nanosystem for biosensing of cholesterol modifying GCE with Au-Pt BNPs with the help of ionic liquid and chitosan (Safavi and Farjami, 2011). COX enzyme was then immobilized onto this modified electrode. The enzyme on reaction with cholesterol produced H_2O_2 as a side product, which was eventually reduced by BNPs present in the sensing matrix. The cholesterol amount was monitored in a dose dependent manner using the fabricated sensor which resulted in low LOD of 10 µM. The BNP mediated sensor designed in this study showed fast response time of < 7s and a sensitivity of 90.7 µA/mM cm^2. In addition to electrochemical sensing of cholesterol, there has also been report on BNP based optical sensing of cholesterol. In one such example, Zhang *et al.* designed Au-Ag BNPs and used them in enzyme based colorimetric biosensing of cholesterol and glucose (Zhang et al., 2016). BNPs were synthesized by subsequent chemical reduction of Au followed by Ag to obtain Ag coated Au core-shell BNPs. COX action on cholesterol produced corresponding amount of H_2O_2 which etched the Ag coating of the Au-Ag BNPs and consequently, stripped the gold core. This resulted in color change and shift in the absorbance maxima of the solution. The biosensor had a wide LR between 0.3 and 300 µM for cholesterol detection and a low LOD of 0.15 µM. Comparing analytical performances of the aforementioned examples, it can be seen that the biosensor incorporating Au-Ag BNPs resulted in lowest LOD for cholesterol detection. This observation signifies that the strategy adopted for biosensor fabrication in this example was very effective and incorporation of Au-Ag BNPs enhanced the analytical performance of the biosensor.

4.2.3 Sensing of organophosphates

Biosensors employing BNPs for the detection of organophosphate, an extremely toxic class of pesticide compounds, are relatively less developed. Of the few available reports, Zhan *et al.* devised an electrochemical biosensor for organophosphate detection by incorporating Au-Pd BNPs (Zhan et al., 2015). They functionalized the GCE with Au-Pd BNP, ionic liquid, graphene, and chitosan. The Au-Pd BNP modified electrode was reported to exhibit less electron transfer resistance *i.e.*, more conductive compared to the same electrode modified with only gold nanoparticles (AuNPs), a mono-NP, indicating the importance of such BNPs in sensitive organophosphate detection. The concentration of the organophosphates was measured by monitoring the degree of inhibition activity of this class of compounds on the enzyme acetylcholine esterase using phorate as a model substrate for this enzyme. This biosensor was reported to give wide LR of 5.0×10^{-16} to 2.5×10^{-13} M and of 4.9×10^{-13} to 9.5×10^{-6} M, with an LOD of 2.5×10^{-16} M, indicating that this sensor can be used to detect organophosphates at extremely low concentrations in real samples. In another study, Upadhyay *et al.*, developed a novel amperometric biosensor for organophosphate pesticide detection based on Au-Pt modified GCE (Upadhyay et al., 2009). The fabrication strategy followed by this group has been shown in **figure 6 (C)**, where the GCE was modified by 3-aminopropyltriethoxy silane (3-APTES) followed by electrodeposition of Au-Pt BNPs. The modified electrode was loaded with acetylcholine esterase/choline oxidase enzyme (bienzyme) whose inhibition was monitored and the proportional amount of organophosphate was calibrated and hence determined. The advantages of using this system were that it enabled detection of multiple organophosphates, such as paraoxon ethyl, sarin, and aldicarb at significantly low concentrations with LOD of 40 nM, 40 µM, and 150 nM and wide LR of 150-200 nM, 40-50 nM, and 40-60 µM, respectively. Another study published by Sreedhar *et al.* demonstrated the use of Au-Cu BNP based biosensor for the detection of chlorpyrifos, another organophosphate (Sreedhar et al., 2015). The detection strategy followed in this report was similar to other conventional organophosphate biosensors where, the sensing was done by monitoring chlorpyrifos inhibition on acetylcholine esterase activity. The fabricated Ag-Cu doped graphene electrode showed better analytical performance than individually doped Ag and Cu graphene electrodes which clearly reiterates the fact of superiority of BNPs over mono-NPs as candidate materials for electrode fabrication. This biosensor was shown to have an LOD of 4×10^{-12} M and a wide LR between 0.01 to 100 nM. It is interesting to note that both the above discussed examples have utilized the inhibition activity of

acetylcholine esterase where two different organophosphates have been tested. There is still ambiguity of the selectivity of multiple organophosphates tested in a mixed sample analysis, therefore work should also be attempted towards developing novel biosensing mechanism, unlike as discussed above, mediating through BNPs.

4.3 Sensing of macromolecules

Among various macromolecules, large polymeric biological molecules like nucleic acid (DNA or RNA), proteins and peptides have been targeted by researchers to be detected by biosensing systems. The target DNA or RNA molecule include specific conserved sequence related to various infectious and non-infectious diseases whereas, target protein may include antigens, epitopes, or biomarkers.

4.3.1 Sensing of nucleic acids

Yola *et al.* had developed a novel electrochemical DNA biosensor based on Fe-Au BNPs (Yola et al., 2014). The 2-aminoethanethiol functionalized graphene electrode was decorated with Fe-Au BNPs followed by immobilization of a standard single stranded DNA oligonucleotide of specific sequence. The LR of the designed sensor was obtained between 1.0×10^{-14} and 1.0×10^{-8} M and an LOD of 2.0×10^{-15} M, indicating the highly sensitive detection of target DNA molecule. The designed biosensor was found to be highly selective towards non-specific as well as single base pair mismatch nucleotides of similar length (17 nucleotides). In another study, Liu *et al.* designed an electrochemical biosensor for the detection of a long non-coding RNA (lncRNA) (Liu et al., 2015), an RNA molecule of more than 200 nucleotides that does not code for any protein but is found to have different gene regulatory functions. This sensor was developed based on Au-Rh BNPs targeting a particular lncRNA: Nuclear paraspeckle assembly transcript1 (NEAT1) for its label free detection. The sensor was fabricated by immobilizing L-Cysteine (Cys) on gold electrode followed by the loading of AuNPs on Cys moieties. Au-Rh BNP bionanoconjugate was designed by wrapping SWCNTs with Au-Rh bimetallic nanospheres and thereafter loading the NEAT1 capture nucleotide sequence and horse radish peroxidase (HRP) on it. This BNP bionanoconjugate was finally adsorbed onto the Cys-AuNP modified gold electrode by hexanethiol, which completed the fabrication of the biosensor electrode. On charging NEAT1, they hybridized with the capture probes, which gave signal due to the reduction of H_2O_2 by HRP and using hemin as electron mediator molecule. Incorporation of Au-

Rh BNPs in sensing probe fabrication had dual advantages: (a) signal amplification due to high catalytic efficiency of Rh and (b) high biocompatibility as result of presence of Au. Additionally, this system also aided in easy loading of the BNP bionanoconjugate on Au-Cys modified gold electrode. The biosensor was reported to be ultrasensitive towards NEAT1 and had an LR of 1 fM/mL to 100 nM/mL and an LOD of 0.8863 fM/mL. To the best of our knowledge, very limited amount of work has been done in this direction, therefore there is an imperative need for development of BNP modified nucleic acid sensors.

4.3.2 Sensing of proteins

Xiao *et al.* developed a biosensor for detection of cardiac troponin 1 (cTnI) (Xiao et al., 2014), a myocardial regulatory protein which is regarded as a high specificity marker for heart injury (Adams et al., 1993). They devised a rather sophisticated strategy to detect cTnI, based on electrochemiluminescence by using Pt-Au BNPs **(figure 7)**. Two types of nanoparticles were prepared: one Au@$RuSiO_2$ nanocomposite and the other Pt-Au BNPs where earlier was used to modify GCE onto which detection antibodies were immobilized. A brilliant architecture of bio-nanoconjugate of Au-Pt BNP comprising glucose dehydrogenase, poly L-histidine (PHP), and reporter antibody was developed to obtain the analytical signals. Using conventional sandwich ELISA like approach, cTnI was trapped between the two nanoparticle layers, then glucose was oxidized and NAD^+ was reduced to NADH. The NADH reduced another species $Ru(phen)_3^{3+}$ to $Ru(phen)_3^{2+}$ and liberate a photon. The $Ru(phen)_3^{2+}$ underwent redox cycling at the electrode and produced amplified analytical signals. Owing to signal amplification, the ultrasensitive detection of cTnI has been achieved with a wide LR between 0.010 ng/mL and 10 ng/mL and an LOD of 3.3 pg/mL. In another report, Sun *et al.* developed an electrochemical biosensor for the detection of carcino-embryonic antigen by using gold electrode and Au-Ag BNPs based on the strategy of sandwiched immunoassay (Sun et al., 2014). In this case, the detection immunoelectrode was modified with AuNPs, whereas the reporter antibodies were linked with Au-Ag BNPs. The target antigen was sandwiched between the two antibodies and the signal was generated due to the action of Au-Ag BNPs linked with reporter antibody which mediated the reduction of H_2O_2 to obtain the analytical signals. This report is again an example of detection of antigen employing an ELISA like technique with the modification of using BNPs instead of enzyme based conventional ELISA. After reviewing the above examples, it can be realized that BNPs, due to

their high catalytic activity, are promising candidates for designing sensors operating on the principle of ELISA but without the use of enzymes. These biosensing techniques are expected to be economical, robust, and possessing higher shelf life, even though uncompromised specificity and selectivity towards the target analyte.

4.4 Sensing of cancerous and bacterial cells

Biosensors targeted at detection of whole cells include several types of cells starting from bacterial origin to mammalian cells. Herein, we have given examples of recent reports on detection systems targeting mammalian as well as bacterial cells. A colorimetric biosensor was developed by Cai *et al.* utilizing Pt-Co BNPs for the detection of cancer cells (Cai et al., 2016) **(figure 8 (A)**). In this work, it has been reported that Pt-Co BNPs possessed magnetic properties and oxidase like catalytic activity due to mutual complementation of the metals. The Pt-Co BNPs were conjugated with aptamers to form nanoconjugates that were used for the detection of MUC1 overexpressing adenocarcinoma cells. The magnetic response of the Pt-Co BNPs enabled separation of the target cells from a population of non-target cells, rendering high specificity of the sensor. The oxidase like activity exhibited by these BNPs was thereby used to reduce H_2O_2, which in turn oxidized TMB to give a characteristic color, whose intensity was proportional to the cancer cell number which was measured at 652 nm. This is another good example of enzyme-less sensing utilizing a BNP in the sensor fabrication. Another report on enzyme-less colorimetric aptasensing of cancer cells Pt-Au BNPs were utilized (Wang et al., 2015). This biosensor employed dual aptamers for MUC1 and $VEGF_{165}$ for the recognition of the target cells. The Pt-Au BNPs were highly catalytic towards TMB oxidation which produced color on the target cell recognition by the aptamers. The biosensor was shown to have an LOD of 10 cells/mL and an LR of 10 to 10^5 cells/mL was obtained showing high sensitivity of the biosensor towards target cells. Another report, came in the same year, described an innovative Cu-Au BNP based colorimetric aptasensing of CCRF-CEM human leukemic cells (Ye et al., 2015). The designed Cu-Au BNPs possessed chemical activity of absorbing iodide which in turn reduced the catalytic effect of iodide on H_2O_2 based TMB oxidation. The Cu-Au BNPs were functionalized with the aptamers and were used to capture the target cells which (cell-BNPs conjugates) were subsequently pelleted out by centrifugation. Very little residual unreacted Cu-Au BNPs were quantified with iodide which consequently produced intense color. The sensor was reported to

have an LOD of 5 cells per 100 µL and a LR between 50 and 500 cells/mL. The sensitivity recorded by this biosensor was better as compared to that of earlier mentioned example most likely due to incorporation of a different bimetallic nanosystem.

The detection of bacterial cells is very important from medical diagnosis as well as environmental monitoring point of view. In case of an infectious disease, early detection can aid in providing medications on time and prevent patients from any serious damage. In order to achieve onsite detection of bacterial cells in a facile experimental setting, Eksi *et al.* developed a core-shell Ag-Au BNP based electrochemical biosensor for detection of *E. coli* cells (Eksi et al., 2015). The strategic fabrication of BNP based biosensor has been shown in **figure 8 (B)**. The bimetallic nanosystem was utilized to immobilize biotinylated anti-*E. coli* antibodies by EDC-NHS coupling. The microwell walls were coated with avidin and biotinylated anti-*E. coli* antibodies were immobilized in the microwell by biotin avidin interaction. Water samples were charged in this microwell and *E. coli* cells present in water got attached with the antibodies. The bio-nanoconjugates with the anti-*E. coli* reporter antibody were then charged on these plates and the *E. coli* cells got sandwiched between the layers of detection antibody and the bimetallic bio-nanoconjugate layers. The LR for *E. coli* detection was recorded between 10 and 10^5 cfu/mL with an LOD of 3 cfu/mL. Another detection system was developed by Jia *et al.*, where core-shell Au-Ag nanorod has been used for the detection of *E. coli* cells (Jia et al., 2015). The detection of the bacteria was done by making use of surface enhanced Raman scattering by the bacterial cells. The biosensor was found to be quick responding and highly sensitive for *E. coli.* In a recent report, *E. coli* was detected with high sensitivity by the aid of Pt-Au BNPs (Jiang et al., 2016). The detection strategy was based on immunochromatography which involved generation of a color signal on detection of cells. The high peroxidase like activity of Pt-Au BNPs helped in further intensification of the color signal and hence, improved the analytical performance by lowering the LOD to 100 cells/mL.

4.5 Sensing of gases and heavy metal

Apart from the target molecules listed above, there are other molecules that have been detected by sensors incorporating BNPs. Mutinati *et al.* devised a CMOS integrated silicon dioxide gas sensor based on BNPs (Mutinati et al., 2014). This group tested three different combinations of BNPs, such as Pd-Au, Pt-Au, and Pd-Pt for performance enhancement of the sensor. They

reported that, of the different metal combinations they tested, Pd-Au BNPs showed enhanced sensitivity to potentially fatal gas, carbon monoxide (CO) and cross reaction with moisture (noise) was completely wiped out. In another report, Choi *et al.* designed a novel gas sensor for detection of nitrogen dioxide (NO_2) using Pt-Pd BNPs (Choi et al., 2013). They decorated tin dioxide (SnO_2) nanowires with Pt-Pd BNPs which were synthesized by radiolysis using γ-radiation. This NO_2 sensor was shown to have both fast response (13s) and quick recovery time (9s) which are due to the incorporation of Pt-Pd BNPs in the sensing matrix. Interestingly, when Pt and Pd mono-NPs were tested separately for NO_2 sensing, slow response was observed. These examples clearly indicate the importance of BNPs in sensor fabrication for the detection of various gaseous molecules. The sensing systems developed could be further extended or modified utilizing other BNPs for various other gaseous molecules detection.

BNP based biosensors have also been utilized for the detection of heavy metal ions in various samples. In one such report, Chen *et al.* developed a sensor for amperometric detection of Pb^{2+} ions using Au-Pd BNPs (Chen et al., 2014). They used DNAzymes, which are artificially constructed DNA having highly specific enzymatic activity but only in presence of a particular metal ion. To achieve this, three single stranded DNA probes (i) capture probe 1, (ii) reporter probe, and (iii) capture probe 2 (say) for wielding the action of DNAzyme were used. The reporter probe was immobilized on SWCNTs decorated with methylene blue (MB-SWCNTs) and connected Au-Fe_2O_3 decorated SiO_2 nanoparticles (Au-Fe_2O_3@ SiO_2). The capture probe 1 was immobilized on three dimensional ordered macroporous (3DOM) Au-Pd modified electrode. The detailed fabrication scheme and detection strategy has been shown in **figure 9**. The advantage of incorporating Au-Fe_2O_3 BNP in biosensing probe fabrication resulted in easy segregation of Au-Fe_2O_3@ SiO_2 by magnetic separation after its cleavage due to DNAzyme action. Besides being highly selective for employing DNAzyme strategy, the LOD reported for this biosensor was extremely low as 10^{-19} M with wide LR between 10^{-17} and 10^{-4} M. Another report on BNP mediated heavy metal detection was published by Gong *et al.* who described a stripping voltammetry-based detection technique for sensing of mercury (Hg(II)) (Gong et al., 2009). They designed Au-Pt BNPs and doped them with the organic polymers to prepare an inorganic BNP-organic nanofiber-based sensing matrix. The analytical performance of the sensor was demonstrated to have an LOD of 0.008 ppb. In another report, Ouyang *et al.* designed Hg-Bi BNPs for multiple detection of three different metals namely, Zn, Cd, and Pb in aqueous samples

(Ouyang et al., 2011). The sensor was fabricated by doping SWCNTs with the Hg-Bi BNPs and the detection was done by anodic stripping voltammetry. The LRs for all the three metals were found to be between 0.5 and 130 μg/L. The LOD were found to be 0.23 μg/L, 0.076 μg/L, and 0.12 ng/L for Zn, Cd, and Pb, respectively. For Pb there was another LR of 5–1100 ng/L. Therefore, this sensor, besides simultaneous detection of Zn and Cd, could detect Pb in ultralow concentrations.

To enable easier comparison of all the examples discussed under Section 4, a summary table (**Table 3)** has been provided with information on composition of the BNPs, sensor design specification, analyte, sensing method applied, competing interference, sensor's analytical performance along with its stability and reproducibility.

5. Conclusions and future prospects

So far, BNPs have been successfully utilized for various biosensing purposes. The multifunctional platform provided by this class of nanoparticles is highly suitable for designing sensors as, the function of two different MeNPs can be obtained in a single hybrid nanosystem. In addition to that, the unique enhanced catalytic, optical, electronic, and magnetic properties shown by these BNPs also make them superior candidates, compared to mono-NPs, for bio/chemical sensing applications. Owing to these properties, BNPs have also been utilized for developing enzyme-less sensors. Despite all the advantages associated with BNPs, there are certain inexplicable insufficiencies in the literature on sensors designed based on these nanoparticles. To the best of our knowledge, no *in vivo* biosensor has been developed utilizing BNPs in the sensing matrix. Thus, the future work should be directed towards clinical validation of the sensor performance which work on BNPs, besides engineering these particles for their novel properties and subsequently utilizing it in the fields where they have not yet been tested. Apart from BNPs, multimetallic nanoparticles like trimetallic, tetrametallic, *etc.* should also be designed and exploited towards designing novel sensors for their potential applications.

Acknowledgements

This work is supported by DST-ECRA research grant (ECR/2016/000100) awarded to Dr. Pranjal Chandra.

Conflict of interest

Authors report no conflict of interest on their parts.

References

Aaron, J.S., Oh, J., Larson, T.A., Kumar, S., Milner, T.E., Sokolov, K.V., 2006. Opt. Express 14(26), 12930-12943.
Abraha, K., 2016. Journal of Physics: Conference Series, p. 012075. IOP Publishing.
Adams, J.r., Bodor, G.S., Davila-Roman, V.G., Delmez, J.A., Apple, F.S., Ladenson, J.H., Jaffe, A.S., 1993. Circulation 88(1), 101-106.
Agrawal, B., Chandra, P., Goyal, R.N., Shim, Y.-B., 2013. Biosens. Bioelectron. 47, 307-312.
Ahmed, J., Sharma, S., Ramanujachary, K.V., Lofland, S.E., Ganguli, A.K., 2009. J. Colloid Interface Sci. *336*(2), 814-819.
Ahmed, S., Ahmad, M., Swami, B.L., Ikram, S., 2016. J. Adv. Res. 7(1), 17-28.
Akdim, O., Demirci, U.B., Miele, P., 2013. Int. J. Hydrog. Energy , *38*(14), 5627-5637.
Alayoglu, S., Eichhorn, B., 2008. J. Amer. Chem. Soc. 130(51), 17479-17486.
Amin, M., Anwar, F., Janjua, M.R.S.A., Iqbal, M.A., Rashid, U., 2012. Int. J. Mol. Sci. 13(8), 9923-9941.
Astruc, D., 2008. Nanoparticles and catalysis. John Wiley & Sons, New Jersey, USA.
Balint, I., You, Z., Aika, K.-i., 2002. Phys. Chem. Chem. Phys. 4(12), 2501-2503.
Bao, Y., Calderon, H., Krishnan, K.M., 2007. J. Phys. Chem. C 111(5), 1941-1944.
Baranwal, A., Chiranjivi, A.K., Kumar, A., Dubey, V.K., Chandra, P., (2018). Sci. Rep. 8(1), 8814, doi: 10.1038/s41598-018-27170-1.
Baranwal, A., Kumar, A., Priyadharshini, A., Oggu, G.S., Bhatnagar, I., Srivastava, A., Chandra, P., 2018a. Int. J. Biol. Macromol. 110, 110-123
Baranwal, A., Mahato, K., Srivastava, A., Maurya, P.K., Chandra, P., 2016. RSC Adv. 6(107), 105996-106010.
Baranwal, A., Srivastava, A., Kumar, P., Bajpai, V.K., Maurya, P.K., Chandra, P., 2018b. Front. Microbiol. 9(422), https://doi.org/10.3389/fmicb.2018.00422.
Barrabés, N., Just, J., Dafinov, A., Medina, F., Fierro, J., Sueiras, J., Salagre, P., Cesteros, Y., 2006. Appl. Catal., B. Environ. 62(1), 77-85.
Bhushan, B., 2010. Springer handbook of nanotechnology. Springer Science & Business Media.
Bhushan, B., 2017. Springer handbook of nanotechnology. Springer, Heidelberg, Berlin.
Boyen, H.-G., Kästle, G., Weigl, F., Ziemann, P., Schmid, G., Garnier, M., Oelhafen, P., 2001. Phys. Rev. Lett. 87(27), 276401-1-276401-4.
Cai, S., Qi, C., Li, Y., Han, Q., Yang, R., Wang, C., 2016. J. Mater. Chem. B 4(10), 1869-1877.
Cao, S., Zhang, L., Chai, Y., Yuan, R., 2013. Talanta 109, 167-172.
Chandra, P., 2016. Nanobiosensors for personalized and onsite biomedical diagnosis. The Institution of Engineering and Technology, London, UK.
Chandra, P., Das, D., Abdelwahab, A.A., 2010. Dig J. Nanomater. Biostruct. 5(2), 363 – 367.
Chandra, P., Koh, W.C.A., Noh, H.-B., Shim, Y.-B., 2012. Biosens. Bioelectron. 32(1), 278-282.
Chandra, P., Noh, H.-B., Pallela, R., Shim, Y.-B., 2015. Biosens. Bioelectron. 70, 418-425.

Chandra, P., Singh, J., Singh, A., Srivastava, A., N Goyal, R., Shim, Y.B., 2013. J. Nanopart. 2013, 1-12.
Chandra, P., Zaidi, S.A., Noh, H.-B., Shim, Y.-B., 2011. Biosens. Bioelectron. 28(1), 326-332.
Chen, K.-J., Lee, C.-F., Rick, J., Wang, S.-H., Liu, C.-C., Hwang, B.-J., 2012. Biosens. Bioelectron. 33(1), 75-81.
Chen, P.C., Mwakwari, S.C., Oyelere, A.K., 2008. Nanotechnol. Sci. Applic. 1, 45-65.
Chen, X., Tian, R., Zhang, Q., Yao, C., 2014. Biosens. Bioelectron. 53, 90-98.
Chen, Y., Cao, H., Shi, W., Liu, H., Huang, Y., 2013. Chem. Comm. 49(44), 5013-5015.
Choi, S.-W., Katoch, A., Sun, G.-J., Kim, S.S., 2013. Sens. Actuators B Chem. 181, 446-453.
Choudhary, M., Yadav, P., Singh, A., Kaur, S., Ramirez- Vick, J., Chandra, P., Arora, K., Singh, S.P., 2016. Electroanalysis 28(10), 2565-2574.
Chung, S., Chandra, P., Koo, J.P., Shim, Y.-B., 2018. Biosens. Bioelectron. 100, 396-403.
Cuenya, B.R., 2010. Thin Solid Films 518(12), 3127-3150.
Darabdhara, G., Sharma, B., Das, M.R., Boukherroub, R., Szunerits, S., 2017. Sens. Actuators B Chem. 238, 842-851.
Eksi, H., Güzel, R., Güven, B., Boyaci, I.H., Solak, A.O., 2015. Electroanalysis 27(2), 343-352.
Félix-Navarro, R.M., Beltrán-Gastélum, M., Reynoso-Soto, E.A., Paraguay-Delgado, F., Alonso-Nuñez, G., Flores-Hernández, J.R., 2016. Renew. Energy, 87, 31-41.
Gan, T., Wang, Z., Shi, Z., Zheng, D., Sun, J., Liu, Y., 2018. Biosens. Bioelectron. 112, 23-30.
Ghodselahi, T., Arsalani, S., Neishaboorynejad, T., 2014. Appl. Surf. Sci. 301, 230-234.
Ghosh Chaudhuri, R., Paria, S., 2011. Chem. Rev. 112(4), 2373-2433.
Ghosh, P., Han, G., De, M., Kim, C.K., Rotello, V.M., 2008a. Adv. Drug Deliv. Rev. 60(11), 1307-1315.
Ghosh, P.S., Kim, C.-K., Han, G., Forbes, N.S., Rotello, V.M., 2008b. ACS nano 2(11), 2213-2218.
Gnanajobitha, G., Paulkumar, K., Vanaja, M., Rajeshkumar, S., Malarkodi, C., Annadurai, G., Kannan, C., (2013). J. Nanostruc. Chem. 3(1), 67.
Gong, J., Zhou, T., Song, D., Zhang, L., Hu, X., 2009. Anal. Chem. 82(2), 567-573.
Gopinath, K., Kumaraguru, S., Bhakyaraj, K., Mohan, S., Venkatesh, K.S., Esakkirajan, M., Kaleeswarran, P., Alharbi, N.S., Kadaikunnan, S., Govindarajan, M., 2016. Microb. Pathog. 101, 1-11.
Gowthaman, N., John, S.A., Tominaga, M., 2017. J. Electroanal. Chem. 798, 24-33.
Goya, G., Berquo, T., Fonseca, F., Morales, M., 2003. J. Appl. Phys. 94(5), 3520-3528.
Gu, X., Lu, Z.-H., Jiang, H.-L., Akita, T., Xu, Q., 2011. J. Amer. Chem. Soc. 133(31), 11822-11825.
Han, Y., Jiang, J., Lee, S.S., Ying, J.Y., 2008. Langmuir 24(11), 5842-5848.
Hierso, J.-C., Feurer, R., Poujardieu, J., Kihn, Y., Kalck, P., 1998. J. Mol. Catal. A: Chem. 135(3), 321-325.
Hori, Y., Otomura, N., Nishida, A., Nishiura, M., Umeno, M., Suetake, I., Kikuchi, K., 2018. J. Am. Chem. Soc, 140(5), 1686-1690.
Ismail, A.A., Bahnemann, D.W., 2011. J. PhyS. Chem. C, 115(13), 5784-5791.
Janasek, D., Vastarella, W., Spohn, U., Teuscher, N., Heilmann, A., 2002. Anal. Bioanal. Chem. 374(7), 1267-1273.
Jiang, T., Song, Y., Wei, T., Li, H., Du, D., Zhu, M.-J., Lin, Y., 2016. Biosens. Bioelectron. 77, 687-694.
Kang, X., Mai, Z., Zou, X., Cai, P., Mo, J., 2007. Anal. Biochem. 369(1), 71-79.

Kato, H., Nakamura, A., Takahashi, K., Kinugasa, S., 2012. Nanomaterials, 2(1), 15-30.
Kelly, K.L., Coronado, E., Zhao, L.L., Schatz, G.C., 2003. ACS Publications. 107(3), 668-677.
Ko, E., Tran, V.-K., Geng, Y., Chung, W.S., Park, C.H., Kim, M.K., Jin, G.H., Seong, G.H., 2017. J. Electroanal. Chem. 792, 72-78.
Ko, S.H., Pan, H., Grigoropoulos, C.P., Luscombe, C.K., Fréchet, J.M., Poulikakos, D., 2007a. Nanotechnology 18(34), 345202, 1-8.
Ko, S.H., Park, I., Pan, H., Grigoropoulos, C.P., Pisano, A.P., Luscombe, C.K., Fréchet, J.M., 2007b. Nano Lett. 7(7), 1869-1877.
Kung, C.-C., Lin, P.-Y., Buse, F.J., Xue, Y., Yu, X., Dai, L., Liu, C.-C., 2014. Biosens. Bioelectron. 52, 1-7.
Lee, C.-C., Chen, D.-H., 2006. Nanotechnology 17(13), 3094-3099.
Leng, J., Wang, W.-M., Lu, L.-M., Bai, L., Qiu, X.-L., 2014. Nanoscale Res. Lett. 9(1), 99, 1-8.
Li, W., Kuai, L., Qin, Q., Geng, B., 2013a. J. Mater. Chem. A, 1(24), 7111-7117.
Li, X., Yao, J., Liu, F., He, H., Zhou, M., Mao, N., Xiao, P., Zhang, Y., 2013b. Sens. Actuators B Chem. 181, 501-508.
Lin, J., Zhou, W., Kumbhar, A., Wiemann, J., Fang, J., Carpenter, E., O'Connor, C., 2001. J. Solid State Chem. 159(1), 26-31.
Liu, F., Xiang, G., Jiang, D., Zhang, L., Chen, X., Liu, L., Luo, F., Li, Y., Liu, C., Pu, X., 2015. Biosens. Bioelectron. 74, 214-221.
Liu, J.-H., Wang, A.-Q., Chi, Y.-S., Lin, H.-P., Mou, C.-Y., 2005. J. Phys. Chem. B 109(1), 40-43.
Liu, X., Astruc, D., 2017. Adv. Mater. 29(16), 1-16.
Mahato, K., Baranwal, A., Srivastava, A., Maurya, P.K., Chandra, P., 2016. Techno-Societal 2016, International Conference on Advanced Technologies for Societal Applications, pp. 421-431. Springer, Cham, Germany.
Mahato, K., Kumar, A., Maurya, P.K., Chandra, P., 2017. Biosens. Bioelectron. 100, 411-428.
Mahato, K., Kumar, S., Srivastava, A., Maurya, P.K., Singh, R., Chandra, P., 2018. Electrochemical Immunosensors: Fundamentals and Applications in Clinical Diagnostics. Handbook of Immunoassay Technologies, pp. 359-414. Academic Press, Elsevier, New York, USA.
Mahato, K., Maurya, P.K., Chandra, P., 2018. 3 Biotech 8(3), 149, https://doi.org/10.1007/s13205-018-1148-8.
Mahato, K., Srivastava, A., Chandra, P., 2017. Biosens. Bioelectron. 96, 246-259.
Mittal, J., Batra, A., Singh, A., Sharma, M.M., 2014. Adv. Nat. Sci. Nanosci. Nanotech. 5(4), 043002, 1-10.
Mizukoshi, Y., Fujimoto, T., Nagata, Y., Oshima, R., Maeda, Y., 2000. J. Phys. Chem. B 104(25), 6028-6032.
Mondal, S., Roy, N., Laskar, R.A., Sk, I., Basu, S., Mandal, D., Begum, N.A., 2011. Colloids Surf. B Biointerfaces, 82(2), 497-504.
Mørup, S., Frandsen, C., Hansen, M.F., 2010. Magnetic properties of nanoparticles. Oxford Handbook of Nanoscience and Technology, , Oxford University Press, UK.
Mutinati, G.C., Brunet, E., Yurchenko, O., Laubender, E., Urban, G., Koeck, A., Steinhauer, S., Siegert, J., Rohracher, K., Schrank, F., 2014. Solid State Device Research Conference (ESSDERC), 2014. 44th European, pp. 78-81. IEEE.
Nasrabadi, H.T., Abbasi, E., Davaran, S., Kouhi, M., Akbarzadeh, A., 2016. Artif. Cells Nanomed. Biotechnol. 44(1), 376-380.

Noh, H.-B., Lee, K.-S., Chandra, P., Won, M.-S., Shim, Y.-B., 2012. Electrochim. acta, 61, 36-43.
Ouyang, R., Zhu, Z., Tatum, C.E., Chambers, J.Q., Xue, Z.-L., 2011. J. Electroanal. Chem. 656(1-2), 78-84.
Pallela, R., Chandra, P., Noh, H.-B., Shim, Y.-B., 2016. Biosens. Bioelectron. 85, 883-890.
Park, J.Y., Zhang, Y., Grass, M., Zhang, T., Somorjai, G.A., 2008. Nano Lett. 8(2), 673-677.
Poole Jr, C.P., Owens, F.J., 2003. Introduction to nanotechnology. John Wiley & Sons, New Jersey, USA.
Prasad, A., Mahato, K., Chandra, P., Srivastava, A., Joshi, S.N., Maurya, P.K., 2016. J. Mol. Eng. Mater. 4(01), 1640004.
Remita, H., Etcheberry, A., Belloni, J., 2003. J. Phys. Chem. B 107(1), 31-36.
Safavi, A., Farjami, F., 2011. Biosens. Bioelectron. *26*(5), 2547-2552.
Sankar, M., Dimitratos, N., Miedziak, P.J., Wells, P.P., Kiely, C.J., Hutchings, G.J., 2012. Chem. Soc. Rev. 41(24), 8099-8139.
Santra, S., Tapec, R., Theodoropoulou, N., Dobson, J., Hebard, A., Tan, W., 2001. Langmuir 17(10), 2900-2906.
Saxena, U., Das, A.B., 2016. Biosens. Bioelectron. 75, 196-205.
Schürmann, S., Wagner, S., Herlitze, S., Fischer, C., Gumbrecht, S., Wirth-Hücking, A., Prölß, G., Lautscham, L., Fabry, B., Goldmann, W., 2016. Biosens. Bioelectron. 81, 363-372.
Singh, A.K., Xu, Q., 2013. Chem. Cat. Chem. 5(3), 652-676.
Sreedhar, N., Kumar, M.S., Krishnaveni, K., 2015. Sens. Actuators B Chem. 210, 475-482.
Sun, G., Ding, Y.-n., Ma, C., Zhang, Y., Ge, S., Yu, J., Song, X., 2014. Electrochim. Acta 147, 650-656.
Suntivich, J., Xu, Z., Carlton, C.E., Kim, J., Han, B., Lee, S.W., Bonnet, N.p., Marzari, N., Allard, L.F., Gasteiger, H.A., 2013. J. Amer. Chem. Soc. 135(21), 7985-7991.
Swihart, M.T., 2003. Curr. Opin. Colloid Interface Sci. 8(1), 127-133.
Tamuly, C., Hazarika, M., Borah, S.C., Das, M.R., Boruah, M.P., 2013. Colloids Surf. B Biointerfaces. 102, 627-634.
Tojo, C., Buceta, D., López-Quintela, M.A., 2017. Catalysts, *7*(2), 68,doi:10.3390/catal7020068.
Toshima, N., Yonezawa, T., 1998. New J. Chem. 22(11), 1179-1201.
Turner, A.P., 2013. Chem. Soc. Rev. 42(8), 3184-3196.
Upadhyay, S., Rao, G.R., Sharma, M.K., Bhattacharya, B.K., Rao, V.K., Vijayaraghavan, R., 2009. Biosens. Bioelectron. 25(4), 832-838.
Vellaisamy, K., Li, G., Ko, C.-N., Zhong, H.-J., Fatima, S., Kwan, H.-Y., Wong, C.-Y., Kwong, W.-J., Tan, W., Leung, C.-H., 2018. Chem. Sci. doi:10.1039/C7SC04798C.
Wang, D., Villa, A., Porta, F., Prati, L., Su, D., 2008. J. Phys. Chem. C 112(23), 8617-8622.
Wang, G.-H., Hilgert, J., Richter, F.H., Wang, F., Bongard, H.-J., Spliethoff, B., Weidenthaler, C., Schüth, F., 2014. Nat. Mater. 13(3), 293-300.
Wang, H., Feng, Z., Del Signore, S.J., Rodal, A.A., Xu, B., 2018. J. Am. Chem. Soc., 140(10), 3505-3509.
Wang, K., Fan, D., Liu, Y., Wang, E., 2015. Biosens. Bioelectron. 73, 1-6.
Wang, W., Vellaisamy, K., Li, G., Wu, C., Ko, C.-N., Leung, C.-H., Ma, D.-L., 2017. Anal. Chem. 89(21), 11679-11684.
Wenderich, K., Mul, G., 2016. Chem. Rev. 116(23), 14587-14619.
Westsson, E., Koper, G.J., (2014). Catalysts, 4(4), 375-396.
Xiao, L., Chai, Y., Wang, H., Yuan, R., 2014. Analyst 139(16), 4044-4050.

Yang, J., Deng, S., Lei, J., Ju, H., Gunasekaran, S., 2011. Biosens. Bioelectron. 29(1), 159-166.
Yola, M.L., Eren, T., Atar, N., 2014. Electrochim. Acta 125, 38-47.
Zaleska-Medynska, A., Marchelek, M., Diak, M., Grabowska, E., 2016. Adv. Colloid Interface Sci. 229, 80-107.Zhan, H., Li, J., Liu, Z., Zheng, Y., Jing, Y., 2015. Anal. Methods 7(9), 3903-3911.
Zhang, X., Chan, K.-Y., 2003. Chem. Mater. 15(2), 451-459.
Zhang, X., Tsuji, M., Lim, S., Miyamae, N., Nishio, M., Hikino, S., Umezu, M., 2007. Langmuir 23(11), 6372-6376.
Zhu, Y., Chandra, P., Ban, C., Shim, Y.B., 2012a. Electroanalysis 24(5), 1057-1064.
Zhu, Y., Chandra, P., Shim, Y.-B., 2012b. Anal. Chem. 85(2), 1058-1064.
Zhu, Y., Chandra, P., Song, K.-M., Ban, C., Shim, Y.-B., 2012c. Biosens. Bioelectron. 36(1), 29-34.

Fig 1: Schematic representation of bimetallic nanoparticle formation. **(A)** core-shell structure formed by the subsequent reduction and **(B)** composite architecture formed by simultaneous reduction of the participating metal ions.

Fig 2: Schematic representation of gamma radiation dependent synthesis of bimetallic nanoparticles. **(A)** low dosage of gamma radiation usually favors core-shell architecture formation. **(B)** high dosage of gamma radiation favors formation of composite bimetallic nanoparticles.

Fig 3: Schematic representation of the comparison between advantages and disadvantages of chemical, physical, and biological BNP synthesis techniques.

Fig 4: Schematic representation of BNPs characterization techniques.

Fig 5: Non-enzymatic colorimetric (optical) detection of H_2O_2 based on the enhanced catalytic property of BNPs, **(A)** shows the oxidation reaction of TMB using Fe-Co BNPs as catalysts, **(B)** shows the relative intensity of the color, which is produced on oxidation of TMB, with Fe-Co BNPs, **(C)** spectral changes of TMB in presence of various catalytic nanoparticles (both monometallic and bimetallic). Reprinted with the permission of Chen *et al.*, copyright (2013) Royal Society of Chemistry.

Fig 6: Fabrication process of electrochemical biosensors for detecting different small molecules by using enhanced catalytic property of BNPs; **(A)** shows probe fabrication using chitosan and Pt-Pd bimetallic nanocomposite for the glucose biosensor, reprinted with permission of Chen *et al.*, copyright (2012) Elsevier; **(B)** shows fabrication of cholesterol biosensor based on Pt-Pd doped graphene, reprinted with permission of Cao *et al.*, copyright (2013) Elsevier; and **(C)** shows the scheme of biosensor fabrication for detection of organophosphates using Au-Pt bimetallic nanoparticles, reprinted with permission of Upadhyay *et al.*, copyright (2009) Elsevier.

Fig 7: Shows the fabrication scheme for electrochemiluminescence based detection of cTnI by using Pt-Au BNPs, reprinted with permission from Xiao *et al.*, copyright (2014) Royal society of Chemistry.

Fig 8: Fabrication of BNP based biosensor for detection of whole cells. **(A)** shows the strategy for simultaneous magnet assisted screening and colorimetric detection of cancer cells using magnetic and catalytic property of Pt-Co BNPs based bio-nanocomposite, reprinted with permission from Cai *et al.*, copyright (2016) Royal Society of Chemistry. **(B)** shows the scheme of Ag-Au bimetallic nanoparticle based immunosensor for *E. coli* detection, reprinted with permission from Eksi *et al.*, copyright (2014) John Wiley and Sons.

Fig 9: Electrochemical detection of Pb^{2+} ions by using magnetic property of the Au-Fe_3O_4 BNPs and DNAzymes, reprinted with permission from Chen *et al*., copyright (2014) Elsevier.

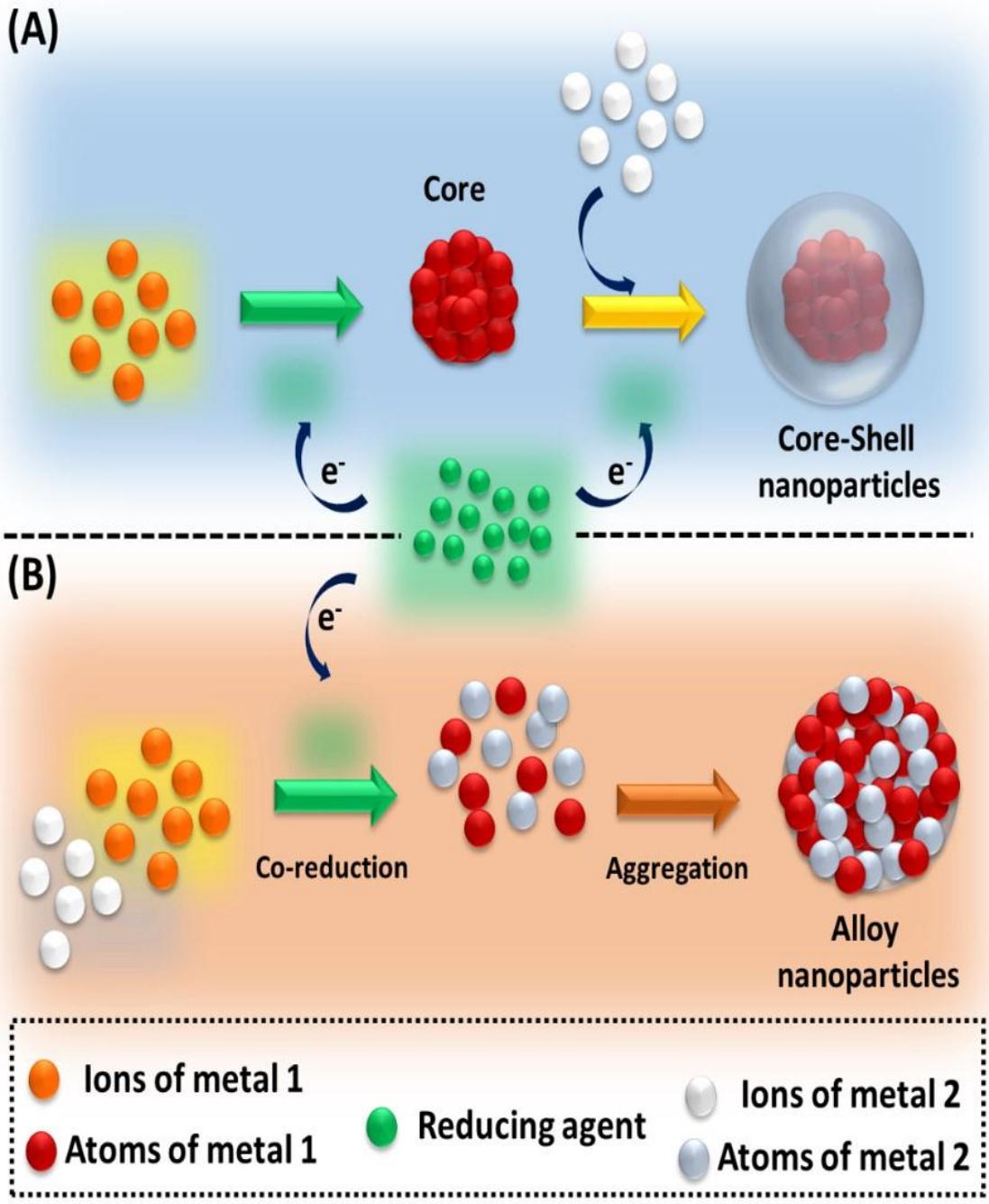
(A)
Core
Core-Shell
nanoparticles
e-
e-
(B)
e-
Co-reduction
Aggregation
Alloy
nanoparticles
Ions of metal 1
Atoms of metal 1
Reducing agent
Ions of metal 2
Atoms of metal 2

Fig. 1

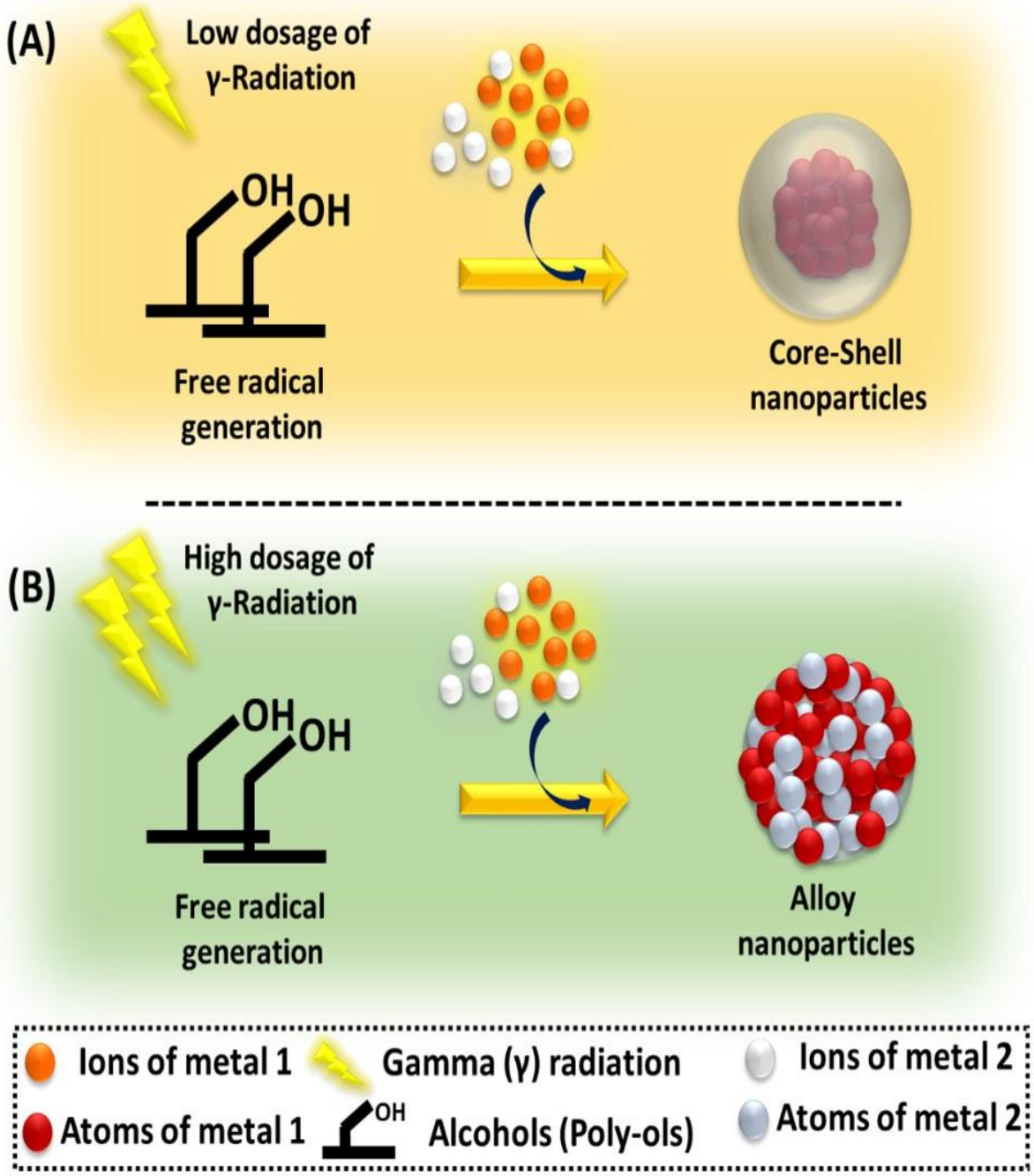
(A)
Low dosage of
γ-Radiation
OH
OH
Free radical
generation
Core-Shell
nanoparticles
(B)
High dosage of
γ-Radiation
OH
OH
Free radical
generation
Alloy
nanoparticles
Ions of metal 1
Gamma (γ) radiation
Ions of metal 2
Atoms of metal 1
OH
Alcohols (Poly-ols)
Atoms of metal 2

Fig. 2

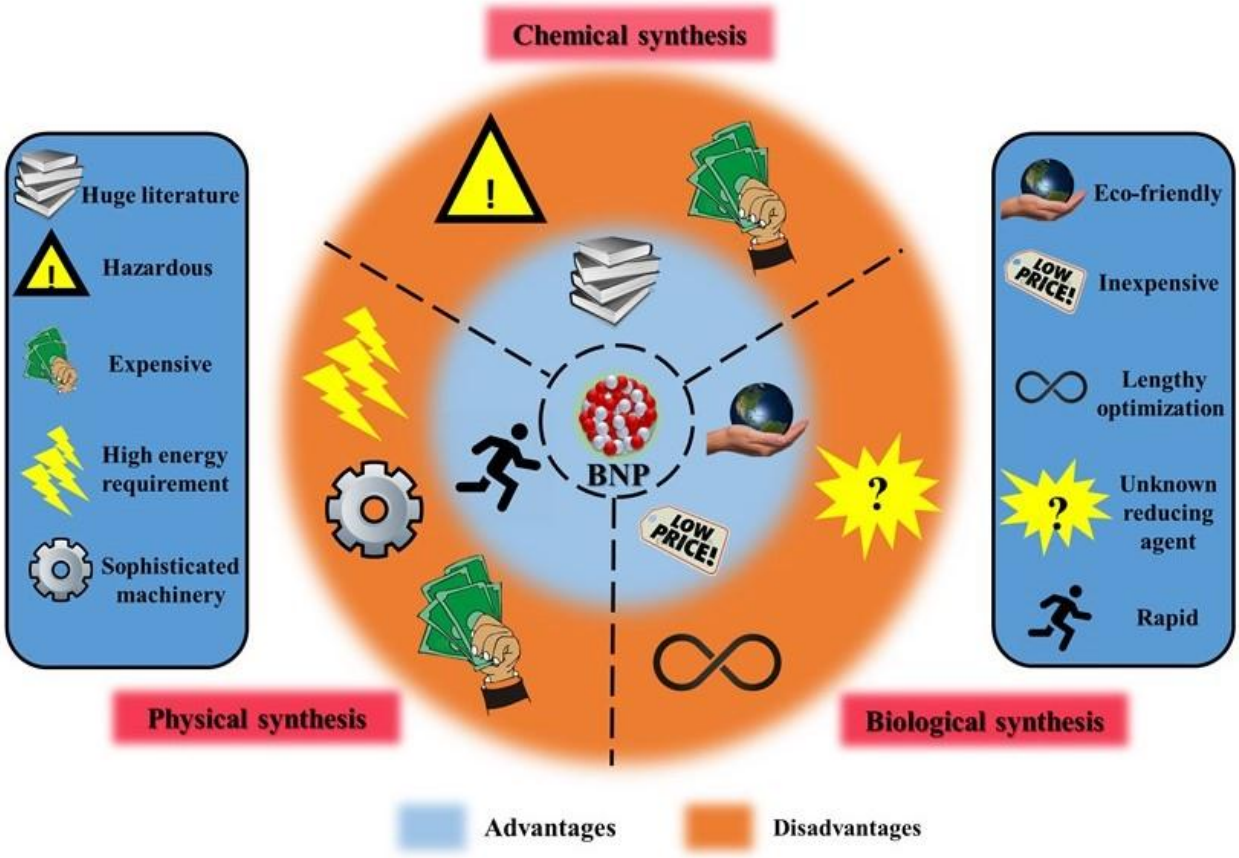

Fig. 3

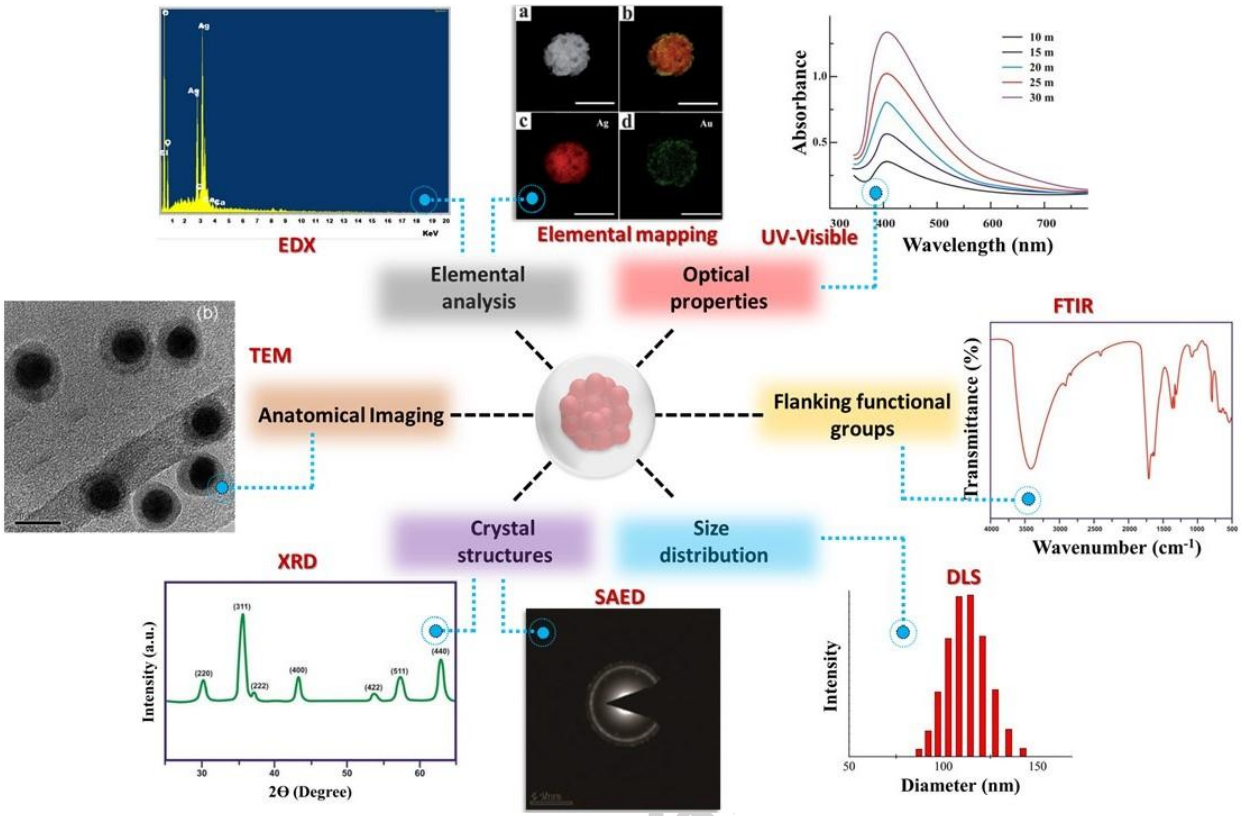

Fig. 4

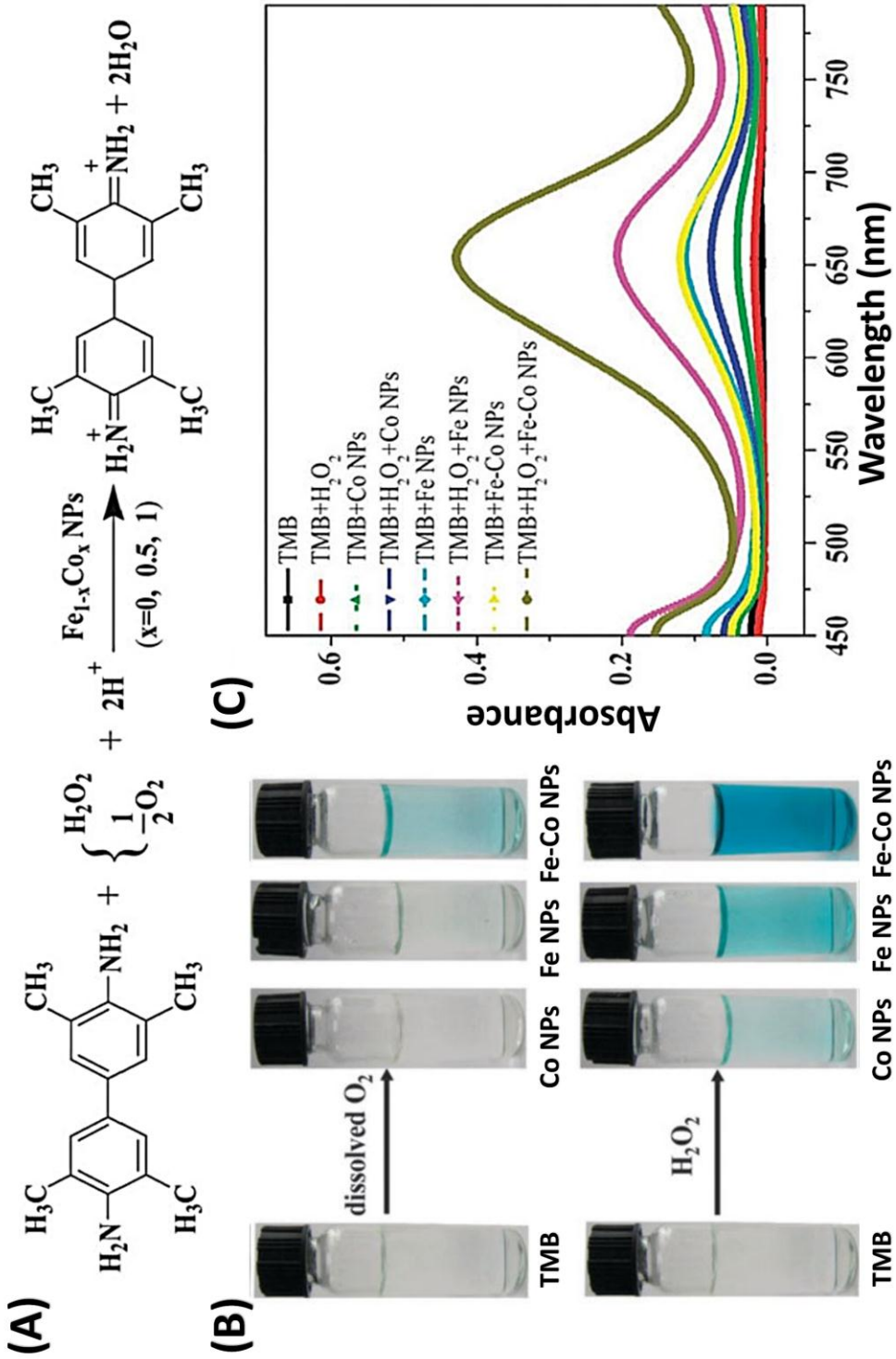
(A)
(B)
(C)
dissolved O2
H2O2
TMB
Co NPs
Fe NPs
Fe-Co NPs
Absorbance
Wavelength (nm)
TMB
TMB+H2O2
TMB+Co NPs
TMB+H2O2+Co NPs
TMB+Fe NPs
TMB+H2O2+Fe NPs
TMB+Fe-Co NPs
TMB+H2O2+Fe-Co NPs

Fig. 5

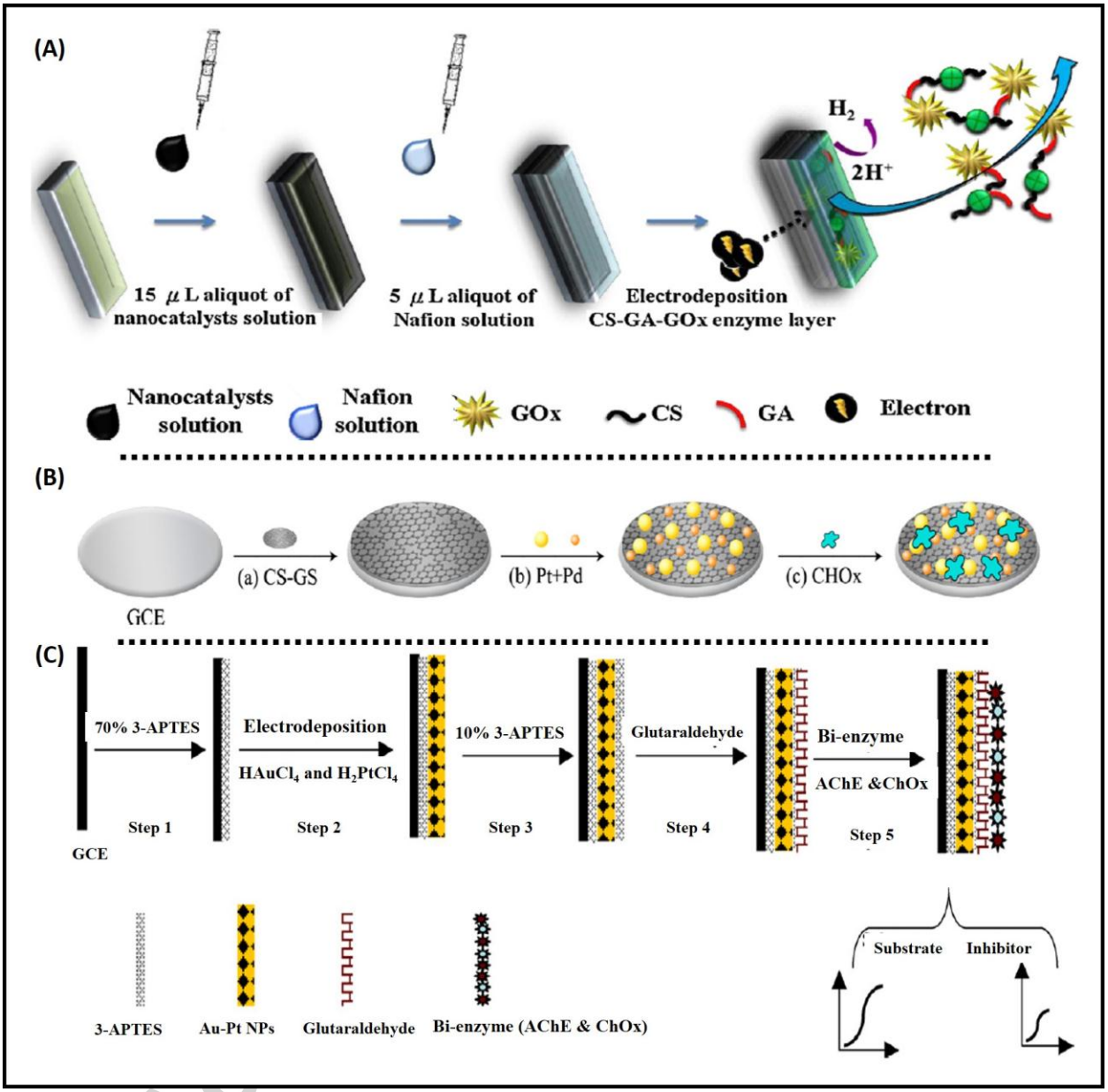
(A)
15 μL aliquot of nanocatalysts solution
5 μL aliquot of Nafion solution
Electrodeposition CS-GA-GOx enzyme layer
H2
2H+
Nanocatalysts solution
Nafion solution
GOx
CS
GA
Electron
(B)
GCE
(a) CS-GS
(b) Pt+Pd
(c) CHOx
(C)
GCE
70% 3-APTES
Step 1
Electrodeposition
HAuCl4 and H2PtCl4
Step 2
10% 3-APTES
Step 3
Glutaraldehyde
Step 4
Bi-enzyme
AChE &ChOx
Step 5
3-APTES
Au-Pt NPs
Glutaraldehyde
Bi-enzyme (AChE & ChOx)
Substrate
Inhibitor

Fig. 6

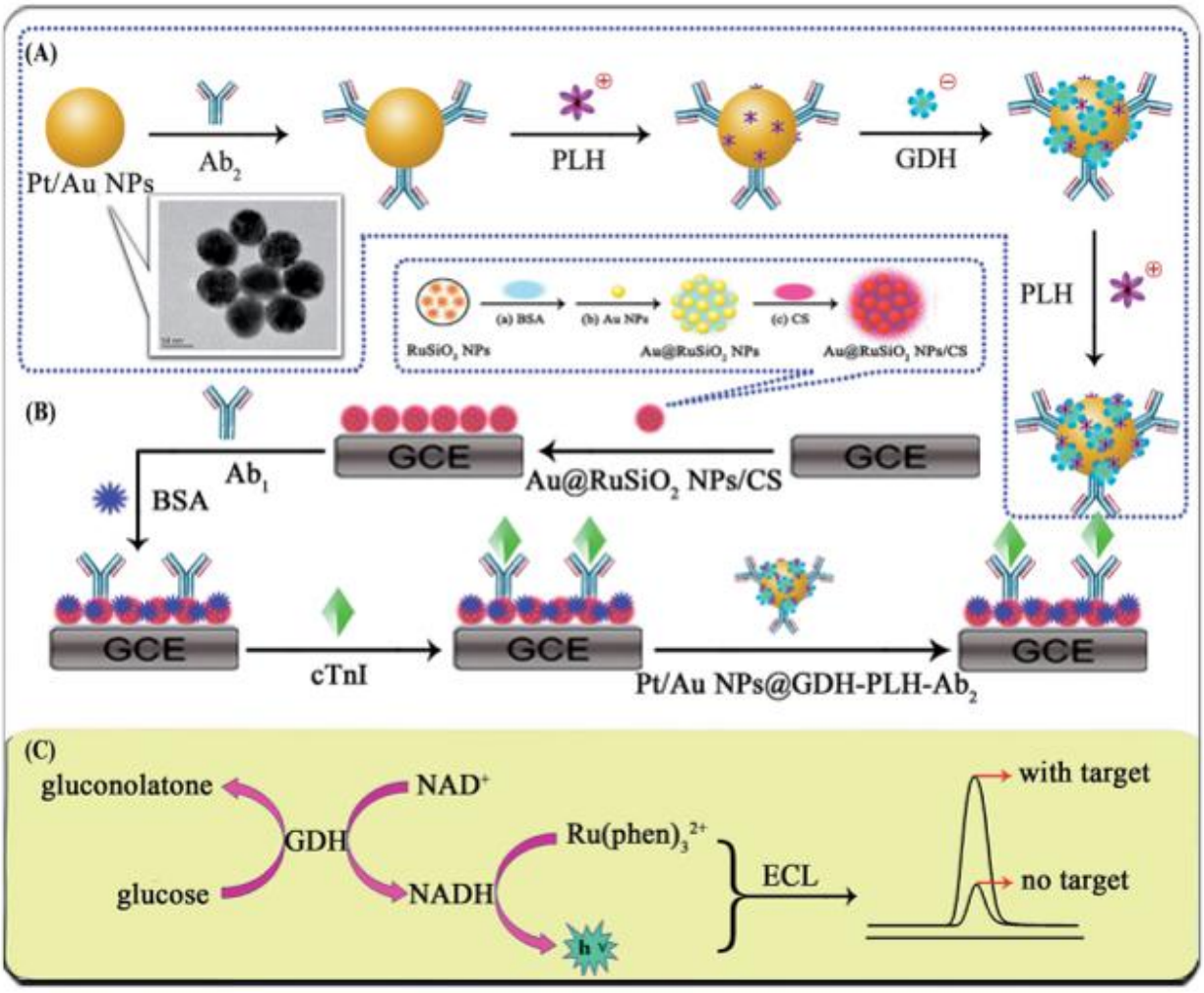

Fig. 7

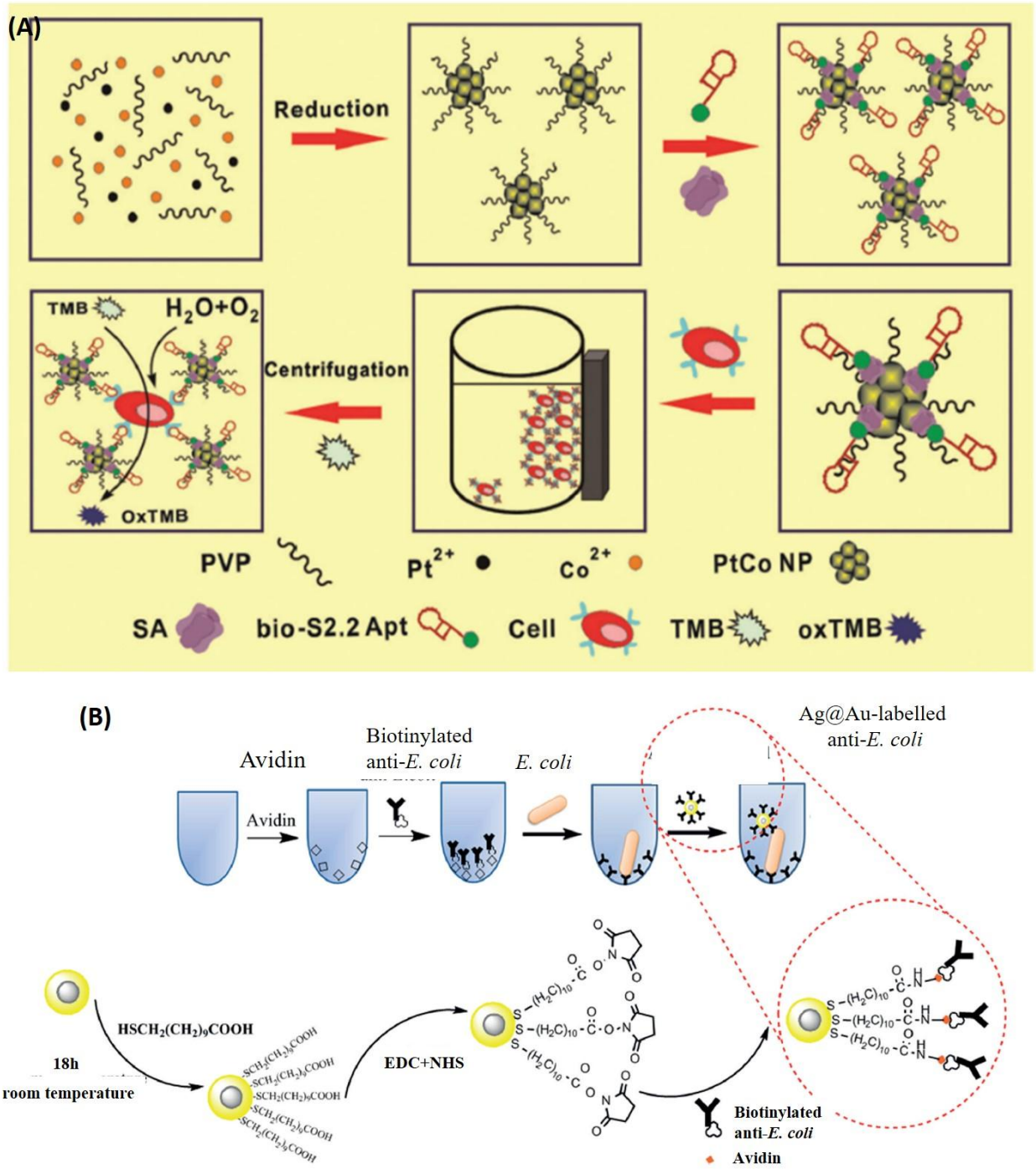
(A)
Reduction
TMB
H_2O+O_2
OxTMB
Centrifugation
PVP
Pt^{2+}
Co^{2+}
PtCo NP
SA
bio-S2.2 Apt
Cell
TMB
oxTMB
(B)
Avidin
Biotinylated anti-E. coli
E. coli
Ag@Au-labelled anti-E. coli
$HSCH_2(CH_2)_9COOH$
18h
room temperature
EDC+NHS
Biotinylated anti-E. coli
Avidin

Fig. 8

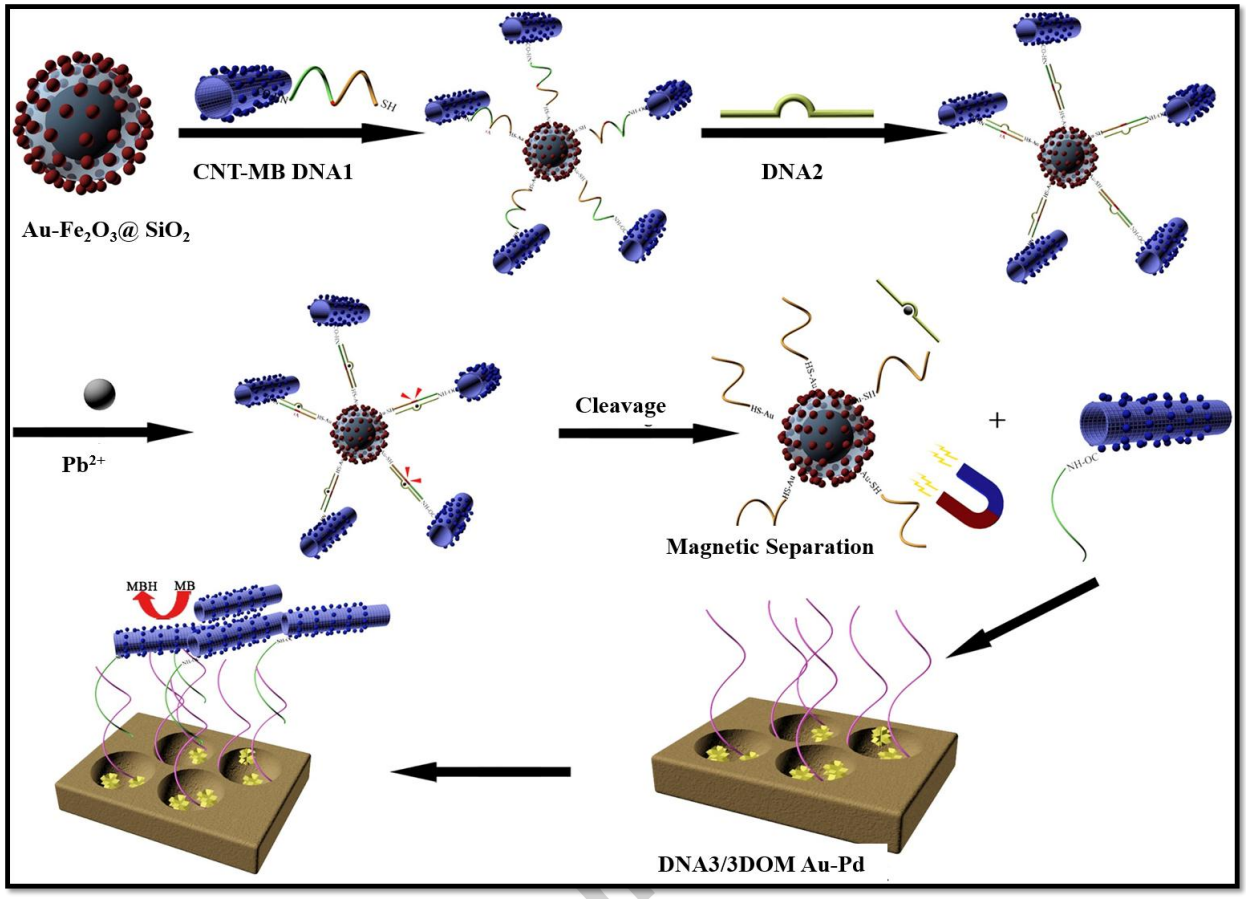

Fig. 9

Table 1: Comparison between advantages and disadvantages of different BNP synthesis techniques.

Synthesis strategy	Advantages	Disadvantages
Chemical	Convenient Lots of data available and many reducing agents have been screened for reduction of different metals	Costly and requires use of hazardous chemicals
Physical	Easy to control the energy dosage Easy to optimize	Requires sophisticated machinery Energy intensive
Biological	Non-toxic Environment friendly Cheap	Optimization is relatively difficult. The actual reducing agent is not always specifically identified.

Table 2: Characterization of nanoparticles via. different techniques.

(a) Necessary characterization		
Characterization	**Information obtained**	**Reference(s)**
X-ray diffraction (XRD)	Crystallinity of the particles can be studied and also the presence of different elements can be determined.	(Gopinath et al., 2016; Lin et al.,2001)
Transmission Electron Microscopy (TEM)	The nanoparticles' morphology and their dispersity can be obtained. Apart from this, average particle size can also be calculated	(Shankar et al.,2004)
Energy Dispersive X-Rays (EDX)	Information about the elemental composition of the particles can be determined which is necessary to understand the bimetallic nature of the particles	(Gnanajobitha et al., 2013)
Selected Area Electron	Information about the crystallinity of the	(Cai et al., 2016)

Diffraction (SAED)	nanoparticles can be obtained.	
Elemental mapping	Visual images of different elements present in the nanoparticles are highlighted by different colors. A concrete evidence of the distribution of elements in BNPs. When elemental mapping is coupled with EDX, the percentage composition of the elements can also be obtained.	(Li et al., 2013a; Wang et al.,2014)
(b) Characterization for elucidation of properties		
Ultraviolet-Visible (UV-Vis) Spectroscopy	Preliminary confirmation of the nanoparticle formation can be obtained, which is further validated by using aforementioned characterization techniques.	(Amin et al., 2012; Ghodselahi et al., 2014)
Fourier Transformed Infra-Red Spectroscopy (FTIR)	Information about the surface chemistry and functional groups (carboxylic, amine, hydroxyl, carbonyl, *etc.*) attached onto the nanoparticle surface can be obtained.	(Gopinath et al., 2016)
Dynamic light scattering (DLS)	Information of surface charge, hydrodynamic size and polydispersity of the nanoparticles can be determined.	(Kato et al., 2012)

Table 3: Summary of different BNP based bio/chemical sensors for the detection of various analytes. *NR = not reported*

BNP composition	**Sensor design specifications**	**Analyte**	**Sensing method / transduction**	**Linear range (LR)**	**Limit of detection (LO**	**Reproducibility/ Stability/ Repeatability**	**Sensitivity**	**Selectivity**	**Real sample analysis**	**Reference**

		system		**D)**						
3.1 Sensing of Hydrogen peroxide										
Au-Ag	Au-Ag decorated SWCNT based microfluidic system	H_2O_2	Electrochemical	0.3-1.8 mM	26.28 µM	Stability = 7 days (RSD = 2.01%) Reproducibility on 24 different sensors (RSD = 0.42 - 3.69%)	13.1 µA/cm^{2}mM	NR	Diluted antiseptic solutions	(Ko et al., 2017)
Au-Ag	Au-Ag /1,6-hexadiamine/ GCE	H_2O_2	Electrochemical	10-120 µM	0.12 µM	NR	NR	NR	NR	(Gowthaman et al., 2016)
Fe-Co	$Fe_{0.5}Co_{0.5}$ NPs/GCE	H_2O_2/ glucose	Optical	0.5-10 µM for glucose	0.01 µM for glucose	Reproducibility on 3 different batches (RSD < 5%)	NR	Sensor is able to distinguish glucose from lactos	Serum for glucose	(Chen et al., 2013)

								e, fructose and maltose.		

3.2 Sensing of small organic molecules

3.2.1 Sensing of Glucose

Au-Pt	GOD/Au-Pt/ CNTs/CS	Glucose	Electrochemical	0.001-7 mM	0.2 µM	Stability = 35 days Reproducibility on 6 different electrodes (RSD = 3.1%) Repeatability (RSD = 2.8%)	8.53 ± 0.09 µA m M^{-1}	Sensor is able to distinguish glucose from uric acid, acetaminophen	Blood and urine samples	(Kang et al., 2007)
Pt-Au	GOD/PtAu / ss-DNA/GR	Glucose	Electrochemical	1-1800 µM	0.3 µM	Stability = 21 days	NR	The sensor is able to distinguish glucose from dopa	Blood sample	(Leng et al., 2014)

								mine, uric acid and ascorbic acid Good selection of glucose		
Pt-Pd	CS-GA-GOx/ Nafion/PtPd-MWCNTs/ GCE	Glucose	Electrochemical	0.062 - 14.07 mM	0.031 mM	Stability = 28 days Reproducibility (RSD = 3.7%)	112 µA/mM.cm^2	from uric acid, ascorbic acid and fructose. Minimal interference	Blood and serum samples	(Chen et al., 2012)
Au-Pd	Graphene oxide/Au-Pd/ GOD	Glucose	Electrochemical	0.5-3.5 mM	6.9 µM	Stability = 14 days Reproducibility on 5 different electrodes (RSD = 9.7%)	266.6 µA/mM cm^2	from uric acid and ascorbic	Blood samples	(Yang et al., 2011)

Ni-Cu	Ni-Cu/TiO_2/Ti	Glucose	Electrochemical	1.0×10^{-5} -3.2×10^{-3} M	5 µM	Stability = 49 days Reproducibility on 6 different electrodes (RSD = 2.96%)	1590.9 µA/mM cm^2	Minimal interference from uric acid and ascorbic acid Good selection of glucose from other simple carbohydrate molecules-maltose, fructose and lactos	Blood samples	(Li et al., 2013)
Cu-Ag	Cu-Ag/rGO nanostructures with glucose oxidase	Glucose	Optical	0.001 - 0.03 mM	3.8 µM	NR	NR		Clinical blood samples	(Darabdhara et al., 2017)

								e.		

3.2.2 Sensing of Cholesterol

Pt-Pd	ChOx/PtPd-CS-graphene/GCE	Cholesterol	Electrochemical	2.2x 10^{-6}-5.2x 10^{-4} M	0.75 µM	Stability = 15-35 days Repeatability after 7 successive measurements (RSD = 4.1%) Reproducibility on 7 different electrodes (RSD = 3.9%)	NR	Minimal interference from uric acid, ascorbic acid and glucose	Food samples like fish oil, margarine, egg and meat.	(Cao et al., 2013)
Au-Pt	ChOx/AuPt-CS-ionic liquid/GCE	Cholesterol	Electrochemical	0.05-6.2 mM and 6.2-11.2 mM	10 µM	Stability= 30 days	90.7 µA/m M cm^2	No interference from ascorbic acid and glucose	Blood serum samples	(Safavi and Farjami, 2011)
Au-Ag	NR	Cholesterol/	Optical	0.3-300	0.15 µM	Reproducibility	NR	Negligible	Urine	(Zhang et

		glucose		µM for chol ester ol	for chol ester ol	(RSD <5.6%)		interfe rence from fructo se, sucros e, lactos e, galact ose, glycin e, methi onine, argini ne, K^+, Na^+	and seru m sam ples	al., 2016)

3.2.3 Sensing of Organophosphate

Au-Pd	AChE/Au–Pd/ IL-GR–CHI/ GCE	Organo phosph ate (Phorat e)	Electr ochem ical	5.0x 10^{-16}- 2.5x 10^{-13} M	2.5x 10^{-16}M	Stability= 15 days Reproduci bility for 6 samples of phorate	NR	No signifi cant interfe rence from Ca^{2+}, Mg^{2+}, Fe^{3+}, glucos e,	Spik ed appl e juic e sam ples	(Zha n et al., 2015)

								citric acid and oxalic acid but phenol, p-nitrophenol, catechol, p-nitroaniline significantly interferes with the detection.		
Au-Pt	Bi-enzyme/Au–Pt /3-APTES/GCE	Organophosphate	Electrochemical	150 – 200 nM (paraoxon ethy	40 nM (sarin), 40 µM (aldicarb), and 150	NR	NR	No interference from electroactive specie	NR	(Upadhyay et al., 2009)

				l), 40–50 nM (sarin), and 40–60 µM (aldicarb)	nM, (paraoxon ethyl)			s like ascorbic acid and uric acid.		
Ag-Cu	Ag-Cu graphene paste electrode	Chlorpyrifos	Electrochemical	0.01-100 nM	$4.0x10^{-12}$ M	Stability= 30 days Repeatedly=10 replicates (RSD=2.8 %)	0.447 µA/nM	Interference from Zn^{2+}, chlordime form amitraz, atrazine and phoxim at manifold high conce	Well water and soil samples	(Sreedhar et al., 2015)

								ntratio n.		
3.3 Sensing of macromolecules										
3.3.1 Sensing of Nucleic acids										
Fe-Au	DNA oligo/ Fe-Au/2-aminoethanethiol/graphene oxide /GCE	DNA	Electrochemical	1x10^{-14} - 1x10^{-8} M	2x10^{-15} M	Stability= 96 hours	NR	Fair selectivity DNA oligos with base mismatches	NR	(Yola et al., 2014)
Au-Rh	Au electrode/ L-Cys/AuNPs / capture probe /hexanethiol /target/hemin	NEAT1 (lncRNA)	Electrochemical	1fM -100 nM	0.8836 fM	Stability= 33 days Reproducibility (RSD < 1.9%)	NR	No significant interference from miRNA-16, β-actin and CEA	Synthetic serum sample	(Liu et al., 2015)
3.3.2 Sensing of Proteins										
Pt-Au	Pt-Au/glucose dehydrogenase– poly (L-histidine)–Ab_2 bioconj	cTnI (protein)	Electrochemical	0.01 -10 ng/mL	3.3 pg/ml	Stable for varying concentrations of cTnI	NR	No significant interference from CEA,	Serum sample	(Xiao et al., 2014)

	ugates					Reproducibility (RSD < 5%)		AFP, IgG and CA15-3		
Au-Ag	Paper working electrode/Au-Ag/antibody	Carcino embryonic antigen (CEA)	Electrochemical	0.001-50 ng/mL	0.3 pg/mL	Stability= 4 weeks maximum Reproducibility (RSD <5.5%)	NR	No interference from CA-125, AFP, PSA	Serum samples	(Sun et al., 2014)
3.4 Sensing of Cancerous and Bacterial cells										
Ag-Au	Avidin/ biotinylated anti-*E.coli* Ab/*E.coli*/ Au-Ag anti-*E.coli* Ab	*E. coli*	Electrochemical	10-10^5 cells /mL	3 cfu/mL	NR	NR	NR	Tap water	(Eksi et al., 2015)
Pt-Co	Poly (vinylpyrrolidone)/Pt-Co/ streptavidine /aptamer	MUC1 + cancer cells	Optical	NR	NR	NR	NR	Cannot distinguish MUC-cell significantly	NR	(Cai et al., 2016)
Pt-	Apt_{MUC1}-	MUC1	Optica	10-	10	Acceptabl	NR	Fairly	Seru	(Wan

Au	$PtAu_{NP}$ /MCF-7/Apt_{VEGF}-MB	and VEG_{165} + cells	l	10^5 cells /mL	cells /ml	e reproducibility		distinguish target cells from other cancer cell types	m sample	g et al., 2015)
Cu-Au	Apt−Cu−Au NPs	CCRF-CEM human leukemic cells	Optical	50-500 cells /mL	5 cells /100 µM	NR	NR	NR	Serum samples	(Ye et al., 2015)
Au-Ag	CTAB/AuAg/ Si chip	*E. coli*	Optical	NR	NR	NR	NR	NR	NR	(Jia et al., 2015)
Pt-Au	Ab1/target/Ab2 Pt-AuBNPs/TMB	*E. coli*	Optical	10^2-10^8 cells /mL	100 cells /mL	NR	NR	NR	NR	(Jiang et al., 2016)

3.5 Sensing of Gases and Heavy metals

Pd-Au/Pt-Au/ Pt-Pd	Pd-Au modified SnO_2	CO	Electrochemical	NR	NR	Increase in response by 13% with Pd-Au modified	NR	Pd-Au modified SnO_2 rendered the syste	NR	(Mutinati et al., 2014)

						SnO_2 enabled lower temperature detection of CO	m highly specific for CO sensing by eliminating cross reactivity from humidity and CO_2			
Pd-Pt	Pt-Pd BNPs decorated SnO_2 nano wires	NO_2	Electrochemical	NR	NR	The sensor had fast response and quick recovery	NR	No significant interference from CO, C_6H_6, and C_7H_8	NR	(Choi et al., 2013)
Au-Pd	Complex fabrication	Pb^{2+}	Electrochemical	10^{-17} and 10^{-4} M	10^{-19} M	High stability till 3 weeks	NR	The sensor was able	Serum sample	(Chen et al., 2014

								to distinguish Pb^{2+} from other divalent heavy metal ions		)
Au-Pt	Au-PtNPs/organic nanofibers/GCE	Hg(II)	Electrochemical	1-6ppb	0.008 ppb	Stability =30days maximum Reproducibility (RSD =1.2%)	7.993 μA/ppb	No significant interference from s Cu(II), Cr(III), Co(II), Fe(II), Zn(II), and Mn(II)	River water sample	(Gong et al.,2009)
Hg-Bi	Hg–Bi/SWNTs/GCE	Zn, Cd, Pb	Electrochemical	0.5 and 130	0.23 μg/L	NR	NR	Ru(III) and Rh(III	River wat	(Ouyang et

	µg/L for all 3 metals and additional LR between 5–1100 ng/L for Pb	(Zn), 0.076 µg/L (Cd) and 0.12 ng/L (Pb)	) shows potential interference for Zn(II)	er sample	al.,2011)

Highlights

- Bimetallic nanoparticle (BNP) synthesis and characterization has been discussed comprehensively.
- Novel techniques of bio/chemical sensor designing incorporating BNPs has been described in detail.
- Sensing of various target molecules by using BNP based bio/chemical sensor has been discussed.
- Comparative analysis of monometallic and BNP based sensor performance has been discussed briefly.